$^{12,13}C(\vec{p},\pi^{\pm})$ reactions at $T_p = 200$ MeV

E. Korkmaz,* S. E. Vigdor, W. W. Jacobs, T. G. Throwe,† and L. C. Bland
Indiana University Cyclotron Facility and Department of Physics, Bloomington, Indiana 47408

M. C. Green‡
Physics Division, Argonne National Laboratory, Argonne, Illinois 60439

P. L. Jolivette
Department of Physics, Hope College, Holland, Michigan 49423

J. D. Brown
Department of Physics, Princeton University, Princeton, New Jersey 08544
(Received 5 April 1989)

The results of a comparative study of the $^{13}C(\vec{p},\pi^{\pm})$ and $^{12}C(\vec{p},\pi^{+})$ reactions at $T_p = 200$ MeV and $30° \leq \theta_{lab}^{\pi} \leq 150°$ are reported. The isospin-dependence of the $NN \rightarrow NN\pi$ processes inside nuclei is investigated by comparing cross sections and analyzing powers for the $^{13}C(p,\pi^{\pm})$ continuum production to those for corresponding $NN \rightarrow NN\pi$ processes in the free case. The comparison favors the dominance of a *quasifree* two-nucleon mechanism in nuclear pion production. Relative populations of discrete final states in the $^{13}C(p,\pi^{\pm})$ spectra are compared, confirming the dominance of the two-nucleon mechanism and suggesting the identification of some high-spin states in the mirror nuclei ^{14}C and ^{14}O. Cross-section and analyzing power angular distributions are presented for discrete final states populated strongly in $^{13}C(p,\pi^{\pm})$ and $^{12}C(p,\pi^{+})$ up to 24 MeV excitation energy. Cross-section data for a number of $^{12,13}C(p,\pi^{+})$ transitions are compared to (p,π^{+}) shell-model calculations employing the elementary $pp \rightarrow d\pi^{+}$ amplitude along with realistic nuclear wave functions. Isolated anomalous features exhibited by strong $^{12,13}C(p,\pi^{+})$ transitions to two highly excited discrete states in ^{13}C and ^{14}C are discussed and alternative possible interpretations for these states are presented.

I. INTRODUCTION

Considerable evidence has accumulated in recent years that $A(p,\pi^{\pm})A+1$ reactions on nuclei are dominated near threshold by a two-nucleon mechanism (TNM), i.e., by $NN \rightarrow NN\pi$ processes occurring within the nucleus.[1-8] Especially strong indications have come from studies of $(\vec{p},\pi^{-})$ reactions,[2-8] where the TNM is able to explain, at least qualitatively, the pronounced selectivity observed for discrete high-spin two-particle one-hole (2p1h) states in the residual nucleus,[3-7] the magnitude and dependence on excitation energy of the continuum cross sections,[7,8] and some features of the cross-section and analyzing power behavior for selected weak transitions.[2]

In contrast to (p,π^{-}), where only a single two-nucleon channel $(pn \rightarrow pp\pi^{-})$ can contribute, three such channels $(pp \rightarrow d\pi^{+}$, $pp \rightarrow pn\pi^{+}$ with pn quantum numbers differing from those of the deuteron, and $pn \rightarrow nn\pi^{+})$ can participate in (p,π^{+}). In each of these (p,π^{+}) channels, a final-state nucleon can refill the vacancy left by the struck target nucleon so that, again in contrast to (p,π^{-}), two-nucleon processes can populate single-particle, as well as two-particle one-hole (2p1h), states with respect to the target nucleus ground state. The single-particle final states may also conceivably be reached by "one-nucleon" or "stripping" processes: $p \rightarrow n\pi^{+}$ in the nuclear field, followed by neutron capture. These features serve to make the interpretation of (p,π^{+}) reactions potentially *more* complicated than that for (p,π^{-}). [Both reactions might be further complicated by contributions from multinucleon processes, in which the projectile interacts explicitly with more than one target nucleon. Multinucleon processes appear important over much of the phase space available to pion absorption on nuclei,[9] but have been shown to be strongly suppressed in (p,π^{-}) reactions near threshold[3,4,7] where the pion mass is converted primarily to kinetic energy of a *single* nucleon.] In order to constrain the interpretation of (p,π^{+}) we have undertaken a comparative study of the $^{13}C(\vec{p},\pi^{\pm})$ reactions, populating the mirror final nuclei ^{14}C and ^{14}O at excitation energies up to $E_x \simeq 25$ MeV. By using a common target nucleus and bombarding energy ($T_p = 200$ MeV) and mirror final nuclei, one can study the (p,π^{+}) and (p,π^{-}) reactions on nuclei under conditions as similar as possible.

It is important to keep in mind, however, that $^{13}C(p,\pi^{+})^{14}C$ and $^{13}C(p,\pi^{-})^{14}O$ are not mirror reactions: the former can involve isospin transfer $\Delta T = \frac{1}{2}$ or $\frac{3}{2}$, while the latter proceeds exclusively via $\Delta T = \frac{3}{2}$. Thus, even if both are dominated by TNM, one may expect significant differences between them in the relative populations of mirror final states and in the behavior exhibited by transitions to the continuum, where amplitudes are averaged over a wide variety of final-state quantum numbers. A

major goal of the present investigation is to see whether the observed (p,π^+)-(p,π^-) differences can be understood within a TNM context as arising from the isospin dependence of the underlying $NN \rightarrow NN\pi$ processes, or whether they instead suggest more fundamental differences between the mechanisms. In particular, cross sections and analyzing powers $[A_y(\theta)]$ for $^{13}C(\vec{p},\pi^{\pm})$ continuum transitions are compared in Sec. III A to those measured or predicted for the corresponding *free* $\vec{N}N \rightarrow NN\pi$ reactions at equivalent c.m. energies.

Cross-section and analyzing power results for $^{13}C(\vec{p},\pi^{\pm})$ transitions to a variety of *discrete* final states are presented in Sec. III B, with emphasis on understanding the qualitative differences in the relative populations of mirror states in a TNM context. This comparison also allows some spectroscopic applications for the $A=14$ nuclei, in which we exploit the known[3,4,7] strong selectivity of (p,π^-) reactions for high-spin 2p1h final states and simple TNM arguments regarding mirror configurations that should be accessible in *both* $^{13}C(p,\pi^{\pm})$. In particular, we discuss our identification of previously unknown 5^- states in ^{14}C and ^{14}O in the light of results from other relevant reaction studies.

While the overall results of our study strongly suggest the dominance of *quasifree* $NN \rightarrow NN\pi$ processes in $(p,\pi^{\pm})$ near threshold, a few features of our data do not seem to be easily explainable within this context. This is the case for $A_y(\theta)$ for a strong $^{13}C(\vec{p},\pi^+)$ transition to a previously unknown state at $E_x=23.2$ MeV in ^{14}C. In order to specifically complement the results for this lone anomalous transition, we have also measured cross sections and analyzing powers for $^{12}C(\vec{p},\pi^+)$ up to $E_x \simeq 25$ MeV, and we have found in that case a similarly anomalous transition at $E_x=21.4$ MeV in ^{13}C. The $^{12}C(\vec{p},\pi^+)$ results for a number of transitions to known discrete states are presented briefly in Sec. III C, while possible interpretations for the two anomalous $^{12,13}C(p,\pi^+)$ transitions to high-lying states are discussed in Sec. III D.

A number of (p,π) theoretical models[10] developed in recent years have thus far been unable to reproduce existing $(p,\pi^{\pm})$ data quantitatively and consistently. As reliable nuclear structure input into $A(p,\pi)A+1$ calculations may be an essential ingredient, one further important goal of the current study is to provide a set of $(\vec{p},\pi^{\pm})$ data to test (p,π) reaction models in a region $(A=14)$ where nuclear wave functions are reasonably well understood from shell-model calculations[11,12] and extensively studied at similar momentum transfers $(q \geq 450$ MeV/$c)$ via electron and pion inelastic scattering.[13,14] Throughout Secs. III B and III C we compare our data for a number of $^{12,13}C(p,\pi^+)$ transitions to recent shell-model calculations[15,16] employing a simplified production model assuming $pp \rightarrow d\pi^+$ dominance. Although crude, this model serves to illustrate the sensitivity of the results to details of the nuclear structure.

II. EXPERIMENTAL PROCEDURE

The measurements for $^{13}C(\vec{p},\pi^{\pm})$ and $^{12}C(\vec{p},\pi^+)$ were performed at the Indiana University Cyclotron Facility (IUCF) using a 200-MeV polarized proton beam with typical polarization ~ 0.8 and intensity on target ~ 200 nA. The pions were detected with the IUCF quadrupole-quadrupole split-dipole (QQSP) magnetic spectrometer,[17] optimized for detecting low-energy pions. The range of pion energy in the present work was 20 MeV $\leq T_\pi \leq 60$ MeV. For the measurements reported here, the spectrometer solid angle was $d\Omega=15$ msr, the momentum range covered was $p_{max}/p_{min}=1.6$, and the pion flight path from target to focal plane was 260 cm. The QQSP focal-plane position and entrance angle for detected pions were measured simultaneously with a vertical wire drift chamber (VDC).[17] The VDC was followed by three plastic scintillators measuring the time of flight (both with respect to the cyclotron rf, as well as between detectors) and energy-loss information used to identify the pions and separate them cleanly from background particles (predominantly electrons or positrons arising from pair production by high-energy photons). In the (p,π^+) measurements, a thin plastic absorber was positioned directly in front of the VDC to stop the large flux of low-energy evaporation protons, having the same magnetic rigidity as the pions, from entering the full detector stack.

The effects of significant magnet aberrations and of reaction kinematics on the pion trajectories through the spectrometer were corrected in software on an event-by-event basis, to construct "virtual" focal-plane spectra with optimal pion energy resolution.[7,17] The overall energy resolution observed was typically ~ 180 keV FWHM (full width at half maximum). The dominant contribution to the resolution arose from the energy spread in the incident proton beam, since beam-line constraints prevented effective dispersion matching for such a highly momentum-mismatched reaction. Details of the QQSP detection system and associated electronics and software are described elsewhere.[7,17]

The $^{13}C(p,\pi^+)$ measurements were made with a 96% enriched, 21.5-mg/cm^2 thick, self-supporting ^{13}C target. For the $^{12}C(p,\pi^+)$ data, an enriched (99.9%) ^{12}C target, 33.2-mg/cm^2 thick was used. Each $^{13}C(\vec{p},\pi^+)$ run was followed by a short $^{12}C(\vec{p},\pi^+)$ run with identical QQSP magnet settings and a target of similar thickness, for purposes of background subtraction. The background from $^{12}C(p,\pi^-)^{13}O$ was negligible since the reaction Q value is ~ 20 MeV more negative than for $^{13}C(p,\pi^-)^{14}O$. The relative positions on the virtual focal plane of π^- peaks corresponding to known low-lying states in ^{13}O and ^{14}O, measured with the same magnet fields, provided a stringent test of the broad-range energy calibration of the (p,π^-) spectra. The reliability of the $^{12,13}C(p,\pi^+)$ energy calibration was tested by measuring $^{10}B(p,\pi^+)^{11}B$ peak positions for a number of final states at several spectrometer field settings. These checks demonstrated that the excitation energies of states populated in the $(p,\pi^{\pm})$ reactions could be extracted from the spectra acquired with a single momentum bite of the spectrometer to an accuracy of ≤ 50 keV over a range of 25 MeV.

Measurements for $^{13}C(\vec{p},\pi^{\pm})$ and $^{12}C(\vec{p},\pi^+)$ transitions to final states up to $E_x \simeq 25$ MeV in ^{14}C, ^{14}O, and ^{13}C, were made at nine laboratory angles spanning the range from 30° to 150°. Peak yields were extracted from

the observed virtual focal-plane spectra after application of a software cut on the pion entrance angle to the spectrometer (to eliminate extreme regions subject to severe aberrations or pole-face cutoffs), correction for the fraction of pions lost during in-flight decay along each pion trajectory, and subtraction of the ^{12}C background [for $^{13}C(p,\pi^+)$]. Dead-time corrections to the yields were monitored with the aid of an electronically generated busy signal and a pulser simulating real focal-plane events, and were typically kept below 10%. The QQSP solid angle, pion decay correction, and detection efficiency (along with the Faraday cup beam integration) were checked as a function of focal-plane position and beam-spot location on target, by reproducing $^{10}B(p,\pi^+)^{11}B$ discrete-state absolute cross sections measured[18] earlier with a different instrument. Based on these calibration measurements, and the $^{12,13}C$ target thickness uncertainty of $\sim 10\%$, we estimate an overall absolute cross-section normalization uncertainty of $\pm 14\%$ for most of the measurements reported here. For the ground-state transitions, which have been studied previously,[2,17] we estimate the cross-section normalization uncertainty to be $\pm 17\%$; the extra contribution arises here because, in order to cover the desired excitation energy region with a single field setting, we had to position the ground-state peaks in a region of the focal plane where the detection efficiency was reduced from the maximum value by $\sim 20\%$ and was falling rapidly. The error bars quoted in this paper reflect contributions from counting statistics, peak fitting, and background subtraction only. The proton beam polarization, typically 80% (73%) for the ^{13}C (^{12}C) data, was measured periodically with a low-energy ($T_p \simeq 15$ MeV) polarimeter and found to be quite stable with time. The absolute error in our beam polarization measurements, and hence the normalization uncertainty in our A_y results, is estimated to be $\pm 3\%$ of the A_y values.

III. EXPERIMENTAL RESULTS AND DISCUSSION

Before proceeding to the discussion of the data, we first summarize some relevant experimental features characterizing the various free $NN \rightarrow NN\pi$ channels, which will constitute an important input to the interpretation of much of the $^{12,13}C(\vec{p},\pi^{\pm})$ data to be presented. The proton bombarding energy used in our measurements is 200 MeV, well below the threshold energy (~ 290 MeV) for pion production in *free NN* collisions. In pion production from nuclei, however, a $NN \rightarrow NN\pi$ process can involve the interaction of the incoming proton with a target nucleon moving with momenta up to the Fermi momentum. Hence, the equivalent bombarding energies in free $NN \rightarrow NN\pi$ reactions induced on stationary nucleons would cover a range up to about 150 MeV above the pion production threshold (i.e., $T_L^{\text{eff}} \leq 440$ MeV). It is thus over this range that we consider free $NN \rightarrow NN\pi$ behavior.

The $NN \rightarrow NN\pi$ reaction cross sections are usually parametrized in terms of isospin-channel cross sections $\sigma_{TT'}$, where T (T') is the isospin of the initial (final) nucleon pair. The correspondence between the charged-pion channels relevant to $(p,\pi^{\pm})$ and these isospin cross sections is

$$pp \rightarrow d\pi^+ \cdots \sigma_{10}^d ,$$

$$pp \rightarrow pn\pi^+ \cdots \sigma_{10}+\sigma_{11} ,$$

$$pn \rightarrow nn\pi^+ \cdots \tfrac{1}{2}(\sigma_{11}+\sigma_{01}) ,$$

$$pn \rightarrow pp\pi^- \cdots \tfrac{1}{2}(\sigma_{11}+\sigma_{01}) .$$

Phase-shift analyses[19] of free $NN \rightarrow NN\pi$ data reveal that within ~ 150 MeV of threshold σ_{10} is an order of magnitude stronger than σ_{11}, while σ_{01} is poorly determined, but appears to be even weaker than σ_{11}. Consequently, for example, the cross section for $pp \rightarrow (pn)_{T=0}\pi^+$ exceeds by a factor of ~ 10–20 that for $pn \rightarrow pp\pi^-$. A similar ratio has been deduced from studies of $\pi^{\pm}$ absorption on *s*-wave nucleon pairs in ^3He at kinetic energies ≤ 100 MeV (Ref. 20).

Other relevant systematics concern the analyzing power (A_y) behavior, which has been measured at a number of bombarding energies for $\vec{p}p \rightarrow d\pi^+$ (Ref. 21) and $\vec{p}p \rightarrow np\pi^+$ (Ref. 22). At energies below 450 MeV, A_y is typically large and negative over most of the angle range,[21] with relatively little difference in the results between the two-body and three-body final states.[22]

A. $^{13}C(\vec{p},\pi^{\pm})$ continuum production

Typical $^{13}C(p,\pi^+)$ and $^{13}C(p,\pi^-)$ broad-range spectra acquired with a single momentum bite of the QQSP spectrometer are shown in Fig. 1. In this section we will focus on the cross-section and analyzing power angular distributions for the continuum regions of these spectra. These distributions are particularly important because they should reflect contributions from a large number of transitions, and thereby represent an average over many nuclear structure effects.

$^{13}C(p,\pi^{\pm})$ double-differential cross-section ($d^2\sigma/d\Omega\, dE$) angular distributions are shown in Fig. 2 for slices of the continuum regions about 1.8-MeV wide and centered at $E_x \simeq 20$, 22, and 25 MeV in ^{14}C, and 19, 21, and 23 MeV in ^{14}O. One notices the stability in angular dependence of $d^2\sigma/d\Omega\, dE(\theta)$ with respect to excitation energy, observed for both (p,π^+) and (p,π^-). This stability reflects the absence of detailed nuclear structure effects in the continuum. For continuum slices of similar excitation energies, the absolute cross sections for (p,π^+) are typically a factor of 10–20 times larger than those for (p,π^-), a ratio consistent with the corresponding ratio $[\sigma_{10}/\frac{1}{2}(\sigma_{11}+\sigma_{01})]$ noted above for near-threshold *free* $NN \rightarrow NN\pi$ reactions. In a TNM picture (p,π^-) reactions on nuclei proceed only through the σ_{11} and σ_{01} channels (via $pn \rightarrow pp\pi^-$), while all (σ_{10}, σ_{11}, and σ_{01}) channels (via $pp \rightarrow d\pi^+$, $pp \rightarrow pn\pi^+$, and $pn \rightarrow nn\pi^+$) can participate in (p,π^+). The distinct angular distribution patterns exhibited by the $^{13}C(p,\pi^+)$ vs $^{13}C(p,\pi^-)$ continuum results may then be simply related to different momentum-transfer dependences of the underlying $NN \rightarrow NN\pi$ processes. A quantitative understanding of the angle dependence of these $A(p,\pi^{\pm})$ cross sections in

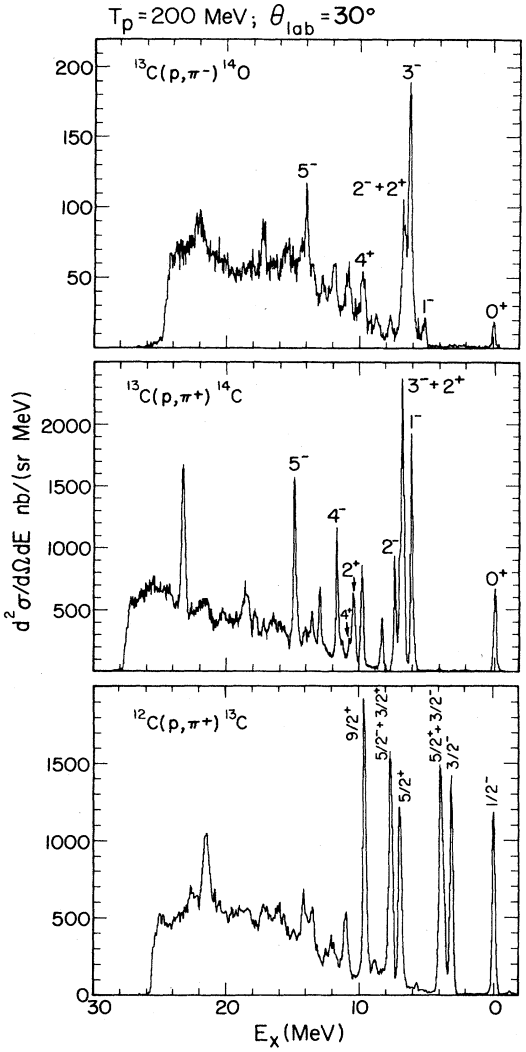

FIG. 1. Typical $^{13}C(p,\pi^+)^{14}C$, $^{13}C(p,\pi^-)^{14}O$, and $^{12}C(p,\pi^+)^{13}C$ spectra, acquired with $T_p=200$ MeV at $\theta_{lab}=30°$. Spin and parity assignments are indicated for some states whose identification is known from previous work or is suggested by the present work.

terms of that of the free $NN\to NN\pi$ cross sections is not trivial, as it would require, even in a plane-wave model, folding the free cross sections with momentum-dependent nuclear form factors.

Analyzing power angular distributions are shown in Fig. 3(b) for two $^{13}C(\vec{p},\pi^+)$ continuum slices. Again, the observed angular distribution shape is insensitive to excitation energy. Furthermore, quite similar results have recently been obtained for other target nuclei.[23] The similarity of these typical $A(\vec{p},\pi^+)$ analyzing powers to experimental results for the $\vec{p}p\to d\pi^+$ process has been noted previously,[1] and is shown in Fig. 3(b) by comparison to $\vec{p}p\to d\pi^+$ results, after appropriate kinematic transformation from the p-p system to the p-^{13}C system. This transformation has been performed[24] assuming that in $^{13}C(p,\pi^+)$ the incoming proton interacts with a moving target nucleon in a *quasifree, head-on* collision, and that the pion four-momentum is not affected by passage through nuclear matter. For given detected pion energy and angle, these assumptions fix the relevant target proton momentum; the relevant laboratory bombarding energy (ranging from ~335 to ~400 MeV) and reaction angle for corresponding $\vec{p}p\to d\pi^+$ data are then deduced by transforming to the target proton rest frame. The corresponding A_y values for $\vec{p}p\to d\pi^+$ are then extracted by interpolating among existing data[21] in the appropriate energy and angle ranges; the width of the cross-hatched band representing $\vec{p}p\to d\pi^+$ in Fig. 3(b) reflects our estimate of the uncertainties involved in this interpolation.

The fact that the simple transformation described leads to the relatively good agreement between $^{13}C(\vec{p},\pi^+)$ and $\vec{p}p\to d\pi^+$ results suggests that the nuclear pion production can be viewed as a *quasifree* two-body process. Furthermore, it indicates the dominance in (p,π^+) reactions of the σ_{10} $NN\to NN\pi$ channel. The growing deviation seen at backward angles in Fig. 3(b) between the nuclear data and the quasifree expectations may be related to the neglect in our simple kinematic transformation of the *full* momentum distribution of the struck proton, and also to the neglect of proton and pion distortions. One should expect distortions, in particular, to become important at the large momentum transfers ($q\geq 600$ MeV/c) corresponding to large angles in Fig. 3, since here the probability of finding sufficiently high-momentum components, even in 2p1h states, becomes quite small.

Quite stable $A_y(\theta)$ distributions are also observed for the different $^{13}C(\vec{p},\pi^-)$ continuum slices considered [see Fig. 3(a)]. Here, significant state-to-state variations in $A_y(\theta)$ observed for $^{13}C(\vec{p},\pi^-)$ transitions to *discrete* final states (discussed in Sec. III B) are apparently averaged over in the case of the continuum. Indeed, continuum portions of $(\vec{p},\pi^-)$ spectra for several other target nuclei[25] exhibit $A_y(\theta)$ strikingly similar to the ^{13}C results, as shown in Fig. 3(a). In view of the conclusion reached in the previous paragraph regarding $(\vec{p},\pi^+)$, it is tempting to interpret the stable observed $A_y(\theta)$ pattern for the $(\vec{p},\pi^-)$ continua as a reflection of the intrinsic $\vec{p}n\to pp\pi^-$ behavior. A comparison analogous to that for (p,π^+) is unfortunately not yet possible. While the first analyzing powers measured for $\vec{p}p\to pp\pi^0$ (σ_{11} channel) have just become available,[26] indicating significantly negative A_y values for bombarding energies ~350–500 MeV, understanding the effect of the σ_{01} term awaits similar $\vec{p}n\to NN\pi^\pm$ analyzing power measurements.

However, a phase-shift analysis of differential cross-section data for the quasifree absorption of π^- by a $^1S_0$ proton pair—using the results of a ^{3}He(π^-,pn) study[27] at $T_\pi=62.5$ MeV—has been recently reported.[28] Five discrete possible phase-shift solutions (constrained by unitarity and np scattering results) were found, yielding five *different* predictions for the *polarization* $P_y(\theta)$ of the *outgoing* nucleons in $\pi^-(pp)_{^1S_0}\to pn$. The analysis concludes that this multiplicity of solutions can therefore be resolved by measurements of $P_y(\theta)$.

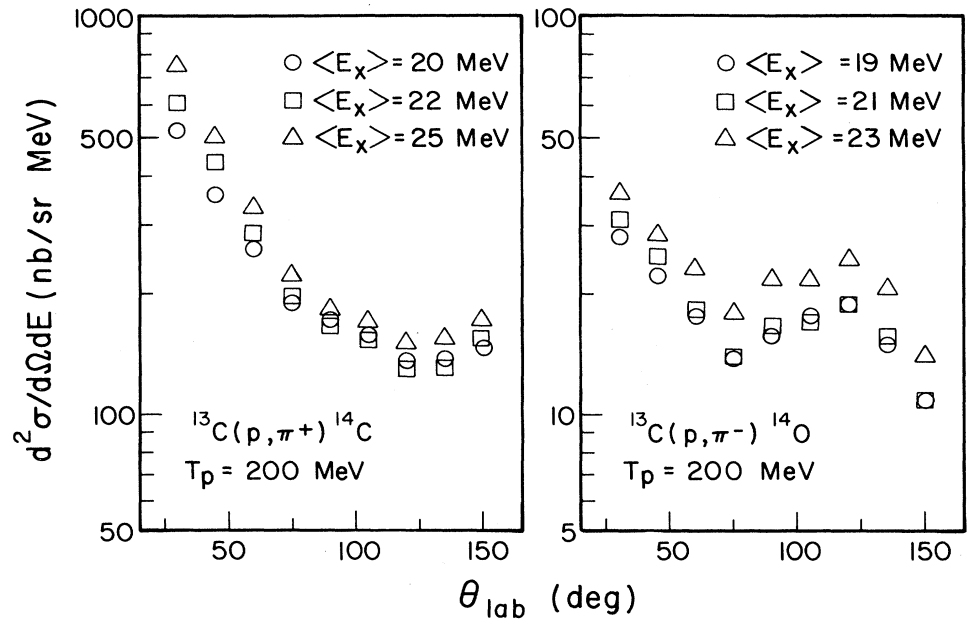

FIG. 2. Double-differential cross-section angular distributions for continuum slices of the $^{13}C(p,\pi^+)$ and $^{13}C(p,\pi^-)$ spectra. The slices are ~1.8 MeV wide (typically) and centered at the excitation energies indicated.

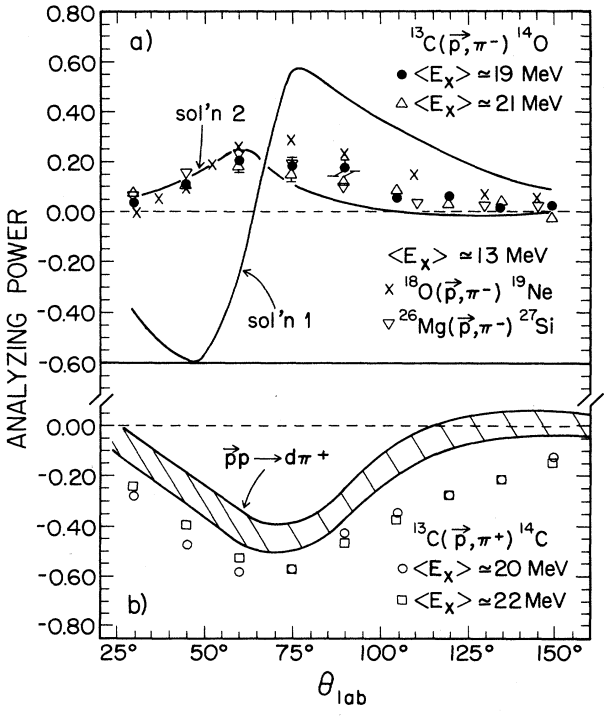

FIG. 3. Comparison of continuum analyzing powers for $^{13}C(\vec{p},\pi^{\pm})$ to experimental results for free $\vec{p}p \rightarrow d\pi^+$ and to phase-shift predictions for $\vec{p}n \rightarrow \pi^-(pp)_{^1S_0}$ (see Sec. III A for details and discussion). The $^{18}O(p,\pi^-)$ and $^{26}Mg(p,\pi^-)$ continuum data shown for comparison are from Ref. 25.

By time-reversal and rotational invariance, $P_y(\theta)$ for $\pi^- pp \rightarrow \vec{p}n$ equals $A_y(\theta)$ for π^- production at the same center-of-mass angle in $\vec{p}n \rightarrow pp\pi^-$. Thus, the same kinematic transformation used in $(\vec{p},\pi^+)$, to compare nuclear $A_y(\theta)$ with free $A_y(\theta)$, has been applied[29] to $pn \rightarrow pp\pi^-$, to see whether the continuum $(\vec{p},\pi^-)$ analyzing powers are compatible with any of these five phase-shift solutions. However, in addition to the assumption of a quasifree two-nucleon π^- production mechanism, other important assumptions underlie the $(\vec{p},\pi^-)$ comparison in Fig. 3(a). First, the low-energy final proton pair in π^- production from a nucleus is expected to be constrained to a $^1S_0$ state, not by nuclear structure (as in the ^{3}He pion absorption case), but rather by the short-range nature of this high-momentum-transfer reaction. The same basic assumption [constraining the np pair in $pp \rightarrow (np)\pi^+$ to a $^3S_1$, $T=0$ state] is implicit in the $(\vec{p},\pi^+)$ comparison of Fig. 3(b) and appears to work well there. Second, the predictions of Ref. 28 are for a single pion energy (62.5 MeV) in $\pi^- pp \rightarrow pn$, and therefore a single laboratory incoming proton energy (412 MeV) in $pn \rightarrow pp\pi^-$. We further assume, therefore, that these $pn \rightarrow pp\pi^-$ predictions can be used without modification over the entire projectile energy range (325–390 MeV) relevant to the quasifree π^- production from ^{13}C in our kinematic transformation. (See Ref. 29 for more discussion.)

The result[29] of applying this transformation to the five different phase-shift solutions obtained indicates that only one of them (solution 2 in Ref. 28) is similar to $A_y(\theta)$ for the $^{13}C(\vec{p},\pi^-)$ continuum, as shown in Fig. 3(a). Here the agreement is excellent at forward angles, deteriorating slightly at large angles in a manner similar to that observed for $(\vec{p},\pi^+)$ in Fig. 3(b). All the other

solutions are very different; one of them (solution 1) is shown for comparison in Fig. 3(a). These qualitatively striking results would appear to support strongly the quasifree TNM for (p,π^-) reactions as well as solution 2 of Ref. 28. It is interesting to note that solution 2 corresponds to the dominance in the $\pi^- pp \to pn$ reaction of the $L_{\pi(pp)}=1$ partial-wave amplitude and a $^3D_1$, $T=0$ final pn state. In the corresponding time-reversed reaction $pn \to pp\pi^-$, this would imply the dominance of the σ_{01} isospin amplitude, in which the ΔN intermediate state is disallowed by isospin conservation. If our analysis is correct, the opposite signs observed (Fig. 3) for $A_y(\theta)$ in $(\vec{p},\pi^+)$ vs $(\vec{p},\pi^-)$ may simply reflect the interchange of spin-singlet and spin-triplet NN states between the dominant amplitudes in the two free cases: $(pp)^1D_2 \to (np)^3S_1\pi^+$, $L_{\pi(np)}=1$ [known to dominate from phase-shift analyses of $pp \to d\pi^+$ (see Ref. 30, for example)] vs $(pn)^3D_1 \to (pp)^1S_0\pi^-$, $L_{\pi(pp)}=1$ (deduced from the above analysis).

In light of the questionable assumptions we have had to make in the $(\vec{p},\pi^-)$ comparison of Fig. 3(a), it is important to test our analysis by direct measurement of $A_y(\theta)$ for $\vec{p}n \to pp\pi^-$ near threshold, concentrating on that region of phase space where the two final protons undergo a $^1S_0$ final-state interaction. The relevance of such a measurement has also been emphasized in Ref. 31. The results of such an experiment could go a long way toward confirming, or casting doubt upon, our present conclusion that the $(\vec{p},\pi^\pm)$ continuum results suggest a dominant role for $NN \to NN\pi$ processes with amplitudes only weakly modified by the nuclear medium. More direct information on the role of ΔN intermediate states in π^- production would also provide a critical constraint on the (p,π) reaction theory.[10]

B. $^{13}C(\vec{p},\pi^\pm)$ transitions to discrete final states

In this section, a number of the observed $(p,\pi^\pm)$ transitions to final ^{14}C and ^{14}O discrete states are examined in detail. We start, however, with a brief, general qualitative comparison of the $^{13}C(p,\pi^\pm)$ spectra, in which the relative strengths of the observed transitions to discrete states and the general trend of their analyzing powers are discussed in comparison with expectations based on simple free $NN \to NN\pi$ considerations. This comparison is now motivated by the apparent dominance in $(p,\pi^\pm)$ of a *quasifree* TNM, as suggested by the continuum results of Sec. III A.

A useful starting point for the $^{13}C(p,\pi^\pm)$ comparison is to review some nuclear structure aspects of the final mirror nuclei ^{14}C and ^{14}O. Reliable and well-tested shell-model calculations exist[11,12] for the $A=14$ nuclei. In addition, shell-model configurations and spin and isospin assignments for some ^{14}C states at high excitation have been suggested[32] by experimental studies of inelastic electron and pion scattering. For orientation, some possible high-spin ($J \geq 3$) mirror configurations in ^{14}C and ^{14}O which are (or are not) accessible in $^{13}C(p,\pi^\pm)$ via interaction of the incoming proton with *one* target nucleon, are listed in Table I. Also listed in this table, for each final configuration, are the possible orbitals of the struck target nucleon in $NN \to NN\pi$ processes and, in cases where it is known, the excitation energy of states believed to be associated with the indicated configuration (even if this is not the dominant configuration for the specified state). The most important point to be noted from Table I for the ensuing discussion is that *not* all pairs of final mirror states can be reached in $^{13}C(p,\pi^\pm)$ via a TNM. For example, the 7^+ configuration listed in Table I could be

TABLE I. Some high-spin mirror configurations in ^{14}C and ^{14}O.

Nucleus	J^π	Configuration	E_x (MeV)	Struck nucleon[a]
^{14}C	3^-	$\|^{12}C\otimes(\nu p_{1/2})(\nu d_{5/2})\rangle$	6.73	any n or p
^{14}O	3^-	$\|^{12}C\otimes(\pi p_{1/2})(\pi d_{5/2})\rangle$	6.27	$p_{1/2}$ neutron
^{14}C	4^+	$\|^{12}C\otimes(\nu d_{5/2})^2\rangle$	10.74	$p_{1/2}$ neutron
^{14}O	4^+	$\|^{12}C\otimes(\pi d_{5/2})^2\rangle$	9.92	$p_{1/2}$ neutron
^{14}C	4^-	$\|^{12}C\otimes(\nu p_{1/2})^2_{0^+}(\nu p_{3/2})^{-1}(\nu d_{5/2})\rangle$	11.7	$p_{3/2}$ neutron
^{14}O	4^-	$\|^{12}C\otimes(\pi p_{1/2})^2_{0^+}(\pi p_{3/2})^{-1}(\pi d_{5/2})\rangle$		none
^{14}C	4^-	$\|^{12}C\otimes(\nu p_{1/2})^2_{0^+}(\pi p_{3/2})^{-1}(\pi d_{5/2})\rangle$	17.3	$p_{3/2}$ proton
^{14}O	4^-	$\|^{12}C\otimes(\pi p_{1/2})^2_{0^+}(\nu p_{3/2})^{-1}(\nu d_{5/2})\rangle$		none
^{14}C	5^-	$\|^{12}C\otimes(\pi p_{3/2})^{-1}(\pi p_{1/2})(\nu p_{1/2})(\nu d_{5/2})\rangle$		$p_{3/2}$ proton
^{14}O	5^-	$\|^{12}C\otimes(\nu p_{3/2})^{-1}(\nu p_{1/2})(\pi p_{1/2})(\pi d_{5/2})\rangle$		$p_{3/2}$ neutron
^{14}C	6^+	$\|^{12}C\otimes(\pi p_{3/2})^{-1}(\pi p_{1/2})(\nu d_{5/2})^2_{4^+}\rangle$		none
^{14}O	6^+	$\|^{12}C\otimes(\nu p_{3/2})^{-1}(\nu p_{1/2})(\pi d_{5/2})^2_{4^+}\rangle$		$p_{3/2}$ neutron
^{14}C	7^+	$\|^{12}C\otimes(\pi p_{3/2})^{-1}(\nu p_{1/2})(\pi d_{5/2})(\nu d_{5/2})\rangle$		$p_{3/2}$ proton
^{14}O	7^+	$\|^{12}C\otimes(\nu p_{3/2})^{-1}(\pi p_{1/2})(\nu d_{5/2})(\pi d_{5/2})\rangle$		none

[a]"Struck nucleon" corresponds to a ^{13}C nucleon with which an incoming proton can interact to form the listed final-state configuration. "None" means that the configuration in question is not accessible via a $NN \to NN\pi$ process. Note that the listed configurations are not necessarily the dominant ones in the specified states (see text for details and discussion).

reached in $^{13}C(p,\pi^+)$ but *not* in $^{13}C(p,\pi^-)$ by interaction with a single target nucleon, since in the latter case one would have to remove neutrons present in *both* $p_{3/2}$ and $p_{1/2}$ orbitals in ^{13}C.

A simple qualitative comparison of the $^{13}C(p,\pi^{\pm})$ spectra of Fig. 1 confirms some of the expectations based on free $NN\rightarrow NN\pi$ results. First, the near-threshold free $\sigma_{10}/(\sigma_{11}+\sigma_{01})\sim 10$ ratio seems to be directly reflected in the $(p,\pi^+)/(p,\pi^-)$ cross-section ratio for comparably excited discrete transitions, as well as for the continuum (as already noted in the preceding subsection). Differences between the two spectra in the *relative* strengths for known mirror final states can also be understood qualitatively in most cases from $NN\rightarrow NN\pi$ expectations. In a (p,π^-) reaction leading to any specific final configuration, the incoming proton is restricted to interact with a target neutron from a specific orbital in effecting a $pn\rightarrow pp\pi^-$ transition. This highly restrictive reaction path results in a very strong selectivity for *high-spin* 2p1h final states, dictated mainly by momentum-matching considerations.[3,4] In (p,π^+), however, target nucleons (both protons and neutrons) from a variety of orbitals can often contribute coherently to, and thereby enhance, transitions to lower-spin final states, causing the high-spin selectivity to be less pronounced. This fact is illustrated in Table II for the transitions to the ground states ($J^\pi=0^+$) and the first excited states ($J^\pi=1^-$) in ^{14}C and ^{14}O. For the (p,π^+) transitions in Table II, even if one restricts attention to the presumably dominant $pp\rightarrow(np)_{T=0}\pi^+(\sigma_{10})$ process, it is still clear that both *s*- and *p*-shell target nucleons can contribute, in contrast to (p,π^-). A simple comparison between the $^{13}C(p,\pi^{\pm})$ spectra in Fig. 1 shows, indeed, that the low-spin states (e.g., 0^+ and 1^-) tend to be more strongly populated relative to higher-spin states (e.g., 3^- and 5^-) in (p,π^+) than in (p,π^-), in agreement with the above qualitative expectation.

Figure 1 also reveals interesting relative population differences among higher-spin states between the (p,π^+) and (p,π^-) spectra. These will be discussed in following subsections with the considerations of Table I as a guideline.

Another major qualitative difference between $^{13}C(p,\pi^+)$ and $^{13}C(p,\pi^-)$ is found in their overall analyzing power behavior. The spin dependence for $^{13}C(\vec{p},\pi^+)$ is illustrated in Fig. 4(a) by spectra at a single laboratory angle (45°). The "spin-sum" spectrum displayed is proportional to the double-differential cross section $(d^2\sigma/d\Omega\,dE)$, while the "spin-difference" spectrum is proportional to the product of the cross section and the analyzing power. It is interesting to note that most of the discrete states, as well as the continuum, have similar A_y values, which are large and negative. Actually, most of the strong discrete-state transitions in $^{13}C(\vec{p},\pi^+)$ exhibit

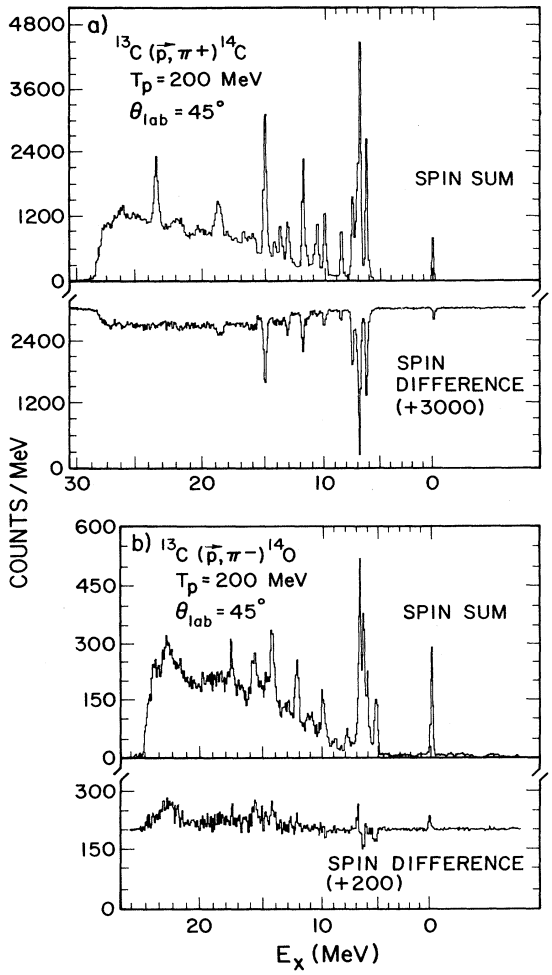

FIG. 4. Spin-sum (proportional to σ) and spin-difference (proportional to σA_y) spectra for $^{13}C(\vec{p},\pi^+)$ and $^{13}C(\vec{p},\pi^-)$ at $\theta_{lab}=45°$.

TABLE II. Dominant ground-state and first-excited-state configurations in ^{14}C and ^{14}O.

J^π	Nucleus	Configuration	E_x (MeV)	2p1h transition[a]	Struck nucleon[a]
0^+	^{14}C	$\lvert^{12}C\otimes(\nu p_{1/2})^2\rangle$	g.s.	$(s_{1/2})^{-1}(s_{1/2})(p_{1/2})$	$s_{1/2}$ p or n
				$(p_{3/2})^{-1}(p_{3/2})(p_{1/2})$	$p_{3/2}$ p or n
				$(p_{1/2})^{-1}(p_{1/2})(p_{1/2})$	$p_{1/2}$ n
0^+	^{14}O	$\lvert^{12}C\otimes(\pi p_{1/2})^2\rangle$	g.s.	$(p_{1/2})^{-1}(p_{1/2})(p_{1/2})$	$p_{1/2}$ n
1^-	^{14}C	$\lvert^{12}C\otimes(\nu p_{1/2})(\nu 2s_{1/2})\rangle$	6.09	$(s_{1/2})^{-1}(s_{1/2})(2s_{1/2})$	$s_{1/2}$ p or n
				$(p_{3/2})^{-1}(p_{3/2})(2s_{1/2})$	$p_{3/2}$ p or n
				$(p_{1/2})^{-1}(p_{1/2})(2s_{1/2})$	$p_{1/2}$ n
1^-	^{14}O	$\lvert^{12}C\otimes(\pi p_{1/2})(\pi 2s_{1/2})\rangle$	5.17	$(p_{1/2})^{-1}(p_{1/2})(2s_{1/2})$	$p_{1/2}$ n

[a]The table shows the variety of $NN\rightarrow NN\pi$ channels and nucleon orbitals that may participate in some $^{13}C(p,\pi^+)$ low-spin transitions, as opposed to the more restricted path for the analogous (p,π^-) transitions.

(see below) $A_y(\theta)$ angular distributions very similar to that for the continuum region studied in Sec. III A. This A_y behavior, therefore, reflects basically the dominance of σ_{10} $NN \rightarrow NN\pi$ processes in nearly all strong (p,π^+) transitions. The seemingly state-independent nature of A_y for most, but not all (as will be discussed later), of the $^{13}C(\vec{p},\pi^+)$ transitions may result partially from averaging over the several transition amplitudes leading to a single final state (e.g., see Table II), thus washing out nuclear structure modifications to the (large) A_y signature of the underlying $NN \rightarrow NN\pi$ process.

In contrast to the stable A_y behavior observed in the case of the (p,π^-) continuum, a sizable state dependence of $A_y(\theta)$ is observed for the $^{13}C(\vec{p},\pi^-)$ transitions to *discrete* final states. This is seen in Fig. 4(b) where spectra analogous to those in Fig. 4(a) have been constructed. Except for the continuum, one notices that there is no clear uniform relationship between the "spin-sum" and "spin-difference" spectra, as there was in Fig. 4(a). In (p,π^-), the angular momentum coupling of the struck nucleon within the target nucleus is typically much more constrained than in (p,π^+) (see Ref. 2). This, coupled with the smaller magnitude of A_y characteristic of the (p,π^-) continuum production (see Sec. III A), presumably allows state-dependent modifications to $A_y(\theta)$, sensitive to the spin-coupling details of the target nucleons involved, to show up more clearly in $(\vec{p},\pi^-)$ than in $(\vec{p},\pi^+)$.

1. 5^- and 4^- states below $E_x = 15$ MeV in ^{14}C and ^{14}O

Following the arguments presented above, we expect that whenever two peaks at similar excitations show up strongly in *both* $^{13}C(p,\pi^+)$ and $^{13}C(p,\pi^-)$ spectra, then they most probably correspond to high-spin 2p1h mirror states that happen to be accessible in both reactions via $NN \rightarrow NN\pi$ processes. This is, for example, the case for the known mirror $J^\pi = 3^-$ states at $E_x = 6.73$ MeV in ^{14}C and 6.27 MeV in ^{14}O (see Fig. 1 and discussion in Sec. III B 4). These are the states most strongly populated at the most forward angle studied (30°). The next most strongly populated pair of states in the $^{13}C(p,\pi^\pm)$ spectra of Fig. 1 are the previously unidentified ones at $E_x = 14.87$ MeV in ^{14}C and 14.15 MeV in ^{14}O. These transitions rapidly become the strongest ones observed at larger angles. Their separation in excitation energy is consistent with that between the known pairs of mirror states at lower excitation. Then, their strong population—together with a number of other features to be discussed below—suggests that these states correspond to the anticipated 5^- mirror configurations listed in Table I [i.e.,

$$|^{12}C \otimes (vp_{1/2})(\pi p_{3/2})^{-1}(\pi p_{1/2})(\nu d_{5/2})\rangle_{5^-}$$

for ^{14}C and

$$|^{2}C \otimes (vp_{1/2})(vp_{3/2})^{-1}(\pi p_{1/2})(\pi d_{5/2})\rangle_{5^-}$$

for ^{14}O].

The 5^- assignment to these states is supported by comparison with results from other reaction studies. The proposed 5^- configurations *cannot* be reached by 1p1h excitations from the ground states of ^{14}C and ^{14}O. This would account for the *absence* of any observed high-spin states at $E_x = 14.87$ MeV in recent $^{14}C(e,e')$ (Ref. 13) and $^{14}C(\pi,\pi')$ (Ref. 14) measurements. On the other hand, the analog 5^-, $T=1$ configuration in ^{14}N,

$$|^{12}C \otimes (vp_{1/2})(\pi p_{1/2})(p_{3/2})^{-1}(d_{5/2})\rangle_{5^-} ,$$

should be excited strongly in inelastic scattering from the 1^+ ground state of ^{14}N via a 1p1h, $(p_{3/2})^{-1}(d_{5/2})$ proton or neutron excitation. Indeed, the strongest state seen[13] in a recent $^{14}N(e,e')$ experiment at backward angles corresponds to an $M4$ transition at just the appropriate excitation energy ($E_x = 16.91$ MeV) for the isobaric analog of the 14.87-MeV state in ^{14}C.

The pion production results for the transition to the 14.87-MeV state in ^{14}C also favor our 5^- assignment. The (p,π^+) cross-section angular distribution for this state is shown in Fig. 5. One notices that $d\sigma/d\Omega(\theta)$ for this transition falls off more slowly with increasing momentum transfer than do distributions for most *known* lower-spin states (See Fig. 8), and is nearly identical in shape to that measured (see Ref. 33 and Sec. III C) for the $^{12}C(p,\pi^+)$ transition to the known high-spin ($\frac{9}{2}^+$) 2p1h state at $E_x = 9.5$ MeV in ^{13}C. The latter $\frac{9}{2}^+$ state is well described[34] as a $d_{5/2}$ neutron coupled to the 2^+, 4.44-MeV state in ^{12}C. Its shell-model wave function is therefore predominantly

$$(\tfrac{1}{2})^{1/2}[|^{12}C \otimes (vp_{3/2})^{-1}(vp_{1/2})(\nu d_{5/2})\rangle] + (\tfrac{1}{2})^{1/2}[|^{12}C \otimes (\pi p_{3/2})^{-1}(\pi p_{1/2})(\nu d_{5/2})\rangle] .$$

Note that only the first of these components can be excited in inelastic scattering via a (neutron) 1p1h transition from the ^{13}C ground state, while only the second component is accessible in $^{12}C(p,\pi^+)$ via the dominant σ_{10} channel. Indeed, this state has been identified[35] in a recent $^{13}C(\pi^\pm,\pi^{\pm'})$ study as an $M4$ *neutron* excitation, and yet is the *strongest* state observed in $^{12}C(p,\pi^+)$. The latter transition, then, involves the same basic rearrangement of nucleons, $(\pi p_{3/2}) \rightarrow (\pi p_{1/2})(\nu d_{5/2})$, as does the postulated transition to the 5^- state in ^{14}C. The two differ only in the presence of the extra $p_{1/2}$ (spectator) neutron in $^{13}C(p,\pi^+)$. The great similarity in cross-section angular distribution between these two transitions (see Fig. 5) is thus one more argument in support of our 5^- assignment to the 14.87-MeV ^{14}C state.

However, a $(\pi p_{3/2})^{-1}(\pi p_{1/2})(\nu d_{5/2})$ transition, leading to a $\frac{9}{2}^+$ final state in $^{12}C(p,\pi^+)$, can lead to *either* 4^- or 5^- final states in $^{13}C(p,\pi^+)$, by virtue of the coupling to the extra $p_{1/2}$ neutron. A natural candidate for such a 4^- state is indeed observed strongly in our $^{13}C(p,\pi^+)$ spectrum (see Fig. 1), at $E_x = 11.67$ MeV. A 4^- state at 11.7 MeV is known from $^{14}C(e,e')$ (Ref. 13) and $^{14}C(\pi,\pi')$ (Ref. 14) studies. Such $M4$ 1p1h excitations from the 0^+ ^{14}C ground state would be associated with 4^- configurations of the type given in Table I, i.e.,

$$|^{12}C \otimes (vp_{1/2})^2(p_{3/2})^{-1}(d_{5/2})\rangle_{4^-} .$$

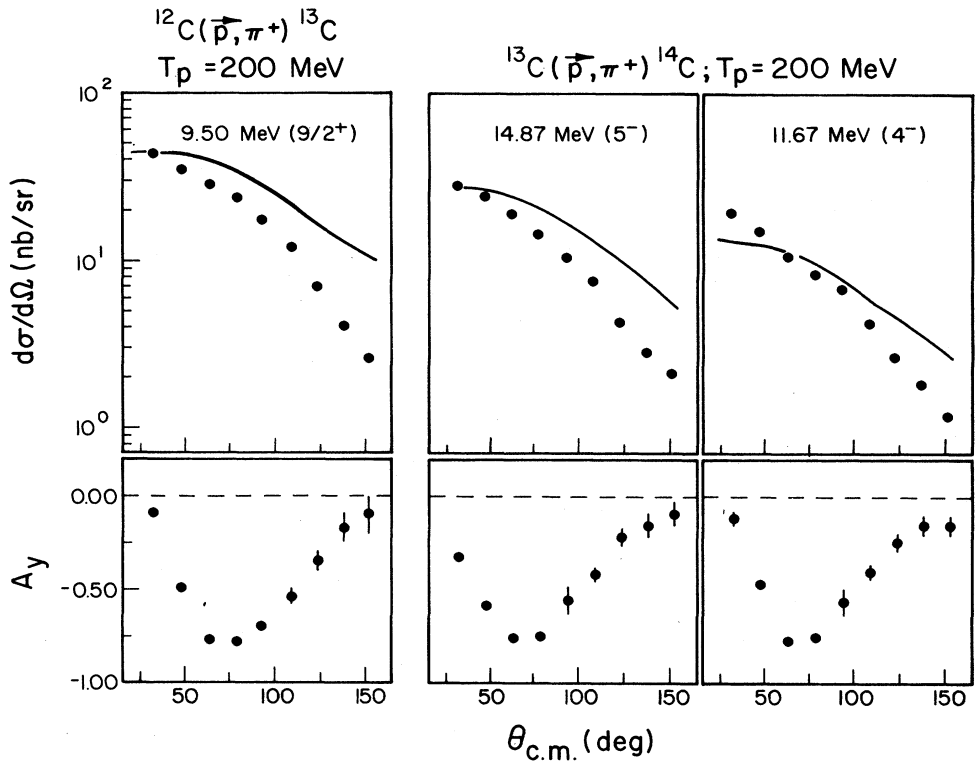

FIG. 5. Cross-section and analyzing power angular distributions for the $^{12}C(p,\pi^+)^{13}C^*$ (9.5 MeV, $\frac{9}{2}^+$), $^{13}C(p,\pi^+)^{14}C^*$ (14.87 MeV, 5^-), and $^{13}C(p,\pi^+)^{14}C^*$ (11.67 MeV, 4^-) transitions. Shown as the solid curves are Kurath's cross-section calculations for these transitions (Refs. 15 and 16). The 5^- assignment for the 14.87-MeV state is from the current work.

The state at 11.7 MeV has been suggested[14] to be predominantly a *neutron* excitation, admixed with a small proton component (the ratio of proton to neutron spectroscopic strengths is estimated to be $\sim\frac{1}{9}$), based on the observed $\sigma(\pi^+,\pi^{+\prime})/\sigma(\pi^-,\pi^{-\prime})$ ratio. The dominant neutron component of the 1p1h excitation populated in inelastic scattering i.e.,

$$|^{12}C\otimes(\nu p_{1/2})^2(\nu p_{3/2})^{-1}(\nu d_{5/2})\rangle_{4^-},$$

is *not* accessible in $^{13}C(p,\pi^+)$ via the strong σ_{10} channel—it can be reached in a TNM only through $pn\rightarrow nn\pi^+$, which is very much weaker in the free case. The proton 1p1h component of the state deduced from (π,π') *can* be populated via σ_{10}, but should still lead to a weak transition because the spectroscopic amplitude is small. Therefore, the large observed strength of the 11.67-MeV state in $^{13}C(p,\pi^+)$ suggests that this state also contains a significant

$$|^{12}C\otimes(\nu p_{1/2})(\pi p_{1/2})(\pi p_{3/2})^{-1}(\nu d_{5/2})\rangle_{4^-}$$

admixture. The previous inelastic scattering studies[13,14] would not have been sensitive to such 2p2h configurations (with respect to $^{14}C_{g.s.}$). The cross-section angular distribution for the 11.67-MeV state is shown in Fig. 5 and is, indeed, almost identical in shape to those for the 9.5-MeV ^{13}C and 14.87-MeV ^{14}C states.

The identification of the 14.87-MeV and 11.67-MeV states is further supported by the absolute (p,π^+) cross sections observed: the *sum* of the cross sections for the $^{13}C(p,\pi^+)$ transitions to these two states in ^{14}C is *equal in magnitude* (within $\sim 10\%$) to that for the $^{12}C(p,\pi^+)$ transition to the $\frac{9}{2}^+$ state. This observation indeed suggests that the $\frac{9}{2}^+$ strength is simply split between the 5^- and 4^- states by the coupling to the extra $p_{1/2}$ neutron in the ^{13}C ground state. Such splitting is approximately consistent with recent simple theoretical calculations[15,16] for $^{13}C(p,\pi^+)$ performed by Kurath. These plane-wave calculations consider the $pp\rightarrow d\pi^+$ reaction as the *only* fundamental process underlying (p,π^+) transitions in nuclei.[36] Their aim is to clarify nuclear structure effects on *relative* transition strengths to particular final states for which shell-model wave functions are available. The predicted[16] $d\sigma/d\Omega(\theta)$ for the $^{13}C(p,\pi^+)$ transitions to the states at 14.87 and 11.67 MeV (using shell-model wave functions for the assumed 5^- and 4^- states), as well as for the $^{12}C(p,\pi^+)$ transition to the $\frac{9}{2}^+$ state in ^{13}C, are shown in Fig. 5 along with the data. One overall normalization factor has been applied to the predicted absolute cross sections, but the relative strengths of the three transitions are given by the calculations and agree reasonably well with the measurements. Agreement with the shape of the angular distributions is only qualitative, as is the case also for other transitions to be discussed below (see

also Ref. 15).

Also shown in Fig. 5 are the analyzing power angular distributions measured for these three $(\vec{p},\pi^+)$ transitions. The great similarity in shape and in magnitude of $A_y(\theta)$ among these states, considered in light of the typical $(\vec{p},\pi^+)$ A_y pattern measured for the continuum [see Fig. 3(b)], is more indicative of the dominance of σ_{10} $NN\rightarrow NN\pi$ processes than of the similarity in configurations between these particular transitions.

The cross-section and analyzing power angular distributions for the strong $^{13}C(p,\pi^-)$ transition to the proposed 5^- state at 14.15 MeV in ^{14}O are shown in Fig. 6. This state has been observed before only in one study[37] of the charge-exchange reaction $^{14}N(^3He,t)^{14}$. One would indeed expect the proposed 5^- configuration to be populated in the charge-exchange reaction by replacing a $p_{3/2}$ neutron by a $d_{5/2}$ proton, starting from the 1^+ ground state of ^{14}N. However, no suggestion for a spin-parity assignment was reported in Ref. 37. Our 5^- assignment to this state, then, is based only on its strong excitation in $^{13}C(p,\pi^-)$ and its mirror lineup with the 14.87-MeV state in ^{14}C. The difference in both $d\sigma/d\Omega(\theta)$ and $A_y(\theta)$ between the $(\vec{p},\pi^+)$ and $(\vec{p},\pi^-)$ results for these presumed mirror states is qualitatively understandable, given the different $NN\rightarrow NN\pi$ amplitudes involved.

A possible candidate (on the basis of excitation energy alone) for an ^{14}O state mirroring the 4^- ^{14}C state at 11.67 MeV is seen at $E_x=10.89$ MeV in the $^{13}C(p,\pi^-)$ spectrum in Fig. 1. As is clear from the considerations in Table I, such a state should be populated in a TNM only through the 2p2h (with respect to $^{14}O_{g.s.}$) admixture analogous to that discussed earlier for the 4^- state in ^{14}C. A state at this excitation was also observed (again, as might be expected) in the $^{14}N(^3He,t)^{14}O$ study of Ref. 37. Its $^{13}C(p,\pi^-)$ cross-section and analyzing power angular distributions are also shown in Fig. 6. The substantial differences between these distributions and those for the presumed 5^- state at 14.15 MeV are surprising in light of the great similarity exhibited for the corresponding (p,π^+) data in Fig. 5. It should be noted that the (p,π^-) peak at 10.89 MeV is rather broad, and may well comprise unresolved transitions.

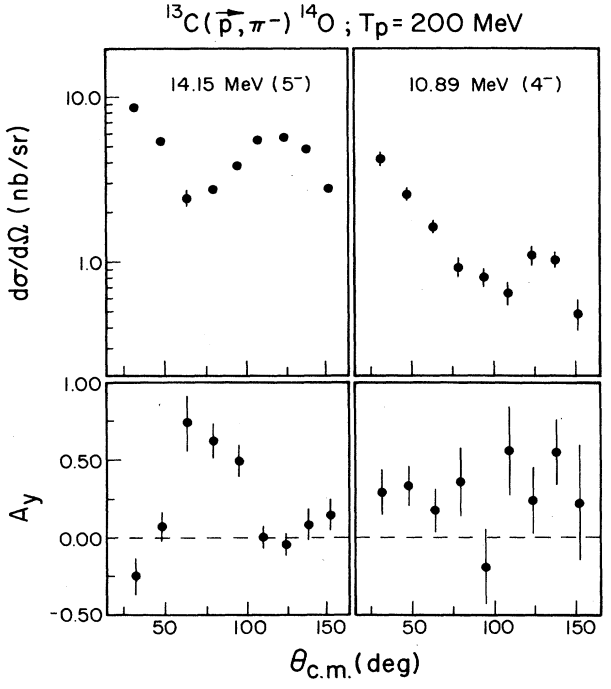

FIG. 6. Cross-section and analyzing power angular distributions for the $^{13}C(p,\pi^-)$ transitions to the 14.15-MeV (5^-) and 10.89-MeV states in ^{14}O. The former spin-parity assignment is suggested by the current results.

2. 4^- states at higher excitation

In addition to the 4^- 11.7-MeV state, the $^{14}C(e,e')$ and $^{14}C(\pi,\pi')$ results[13,14] also suggest another strong 4^- excitation at $E_x=17.3$ MeV. No appreciable peak at this excitation shows up in any of our $^{13}C(p,\pi^+)$ spectra (see Fig. 1). The 1p1h component of this state is believed to be an almost pure $(p_{3/2})^{-1}(d_{5/2})$ *proton* excitation from the ground state of ^{14}C, on the basis of the pion-scattering results.[14] Such a configuration would be expected (see Table I) to be strongly populated in $^{13}C(p,\pi^+)$ via interaction with a $p_{3/2}$ target *proton*. The absence of this state in (p,π^+) is therefore surprising, and suggests possibly a cancellation with an amplitude arising from 2p2h admixtures in the state. This conjecture is not supported by shell-model wave functions: Kurath's calculations[16] predict for this 17.3-MeV state a $^{13}C(p,\pi^+)$ cross-section magnitude about 60% of that for the 4^- state at 11.67 MeV.

The latter calculations also predict a (p,π^+) transition to another 4^- state at $E_x\simeq 18.5$ MeV (not observed in the electron or pion inelastic scattering), with a strength almost equal to that predicted for the 17.3-MeV state. Interestingly, a strong (broad) peak at $E_x=18.53$ MeV is indeed observed in our $^{13}C(p,\pi^+)$ spectra (see Fig. 1). This state has not been seen in any previous study. Its $(\vec{p},\pi^+)$ cross-section and analyzing power angular distributions are shown in Fig. 7, where one notes the typical $(\vec{p},\pi^+)$ $A_y(\theta)$ distribution and $d\sigma/d\Omega$ varying even more slowly with angle than for the 4^- and 5^- states considered in Fig. 5. The cross section for the 18.53-MeV state is about the same (at forward angles) as that for the 4^- 11.67-MeV state, raising the possibility that the (p,π^+) 4^- strength predicted by Kurath for *both* the 17.3 and 18.5-MeV states is concentrated in the one broad state observed at 18.53 MeV.

Finally, the known[13,14] 4^-, $T=2$ state at $E_x=24.3$ MeV in ^{14}C is absent in our $^{13}C(p,\pi^+)$ spectrum (see Fig. 1). This absence is in agreement with the presumed dominance of σ_{10} $NN\rightarrow NN\pi$ processes in (p,π^+): a $T=2$ final state can be reached in $^{13}C(p,\pi^+)$ *only* via $\Delta T=\frac{3}{2}$ transitions, to which the σ_{10} channels *cannot* contribute (since the final *np* pair is coupled to $T=0$).

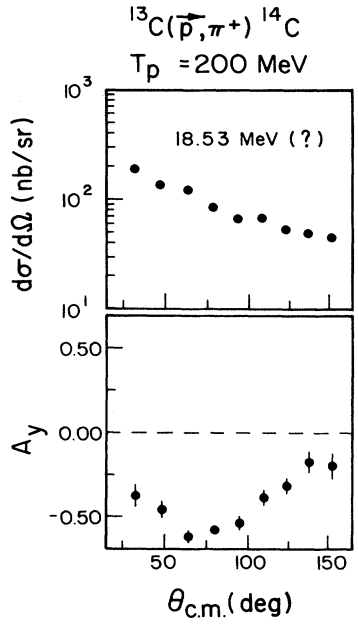

FIG. 7. Cross-section and analyzing power angular distributions for the $^{13}C(p,\pi^+)$ transition to the ^{14}C state at 18.53 MeV. See Sec. III B 2 for discussion.

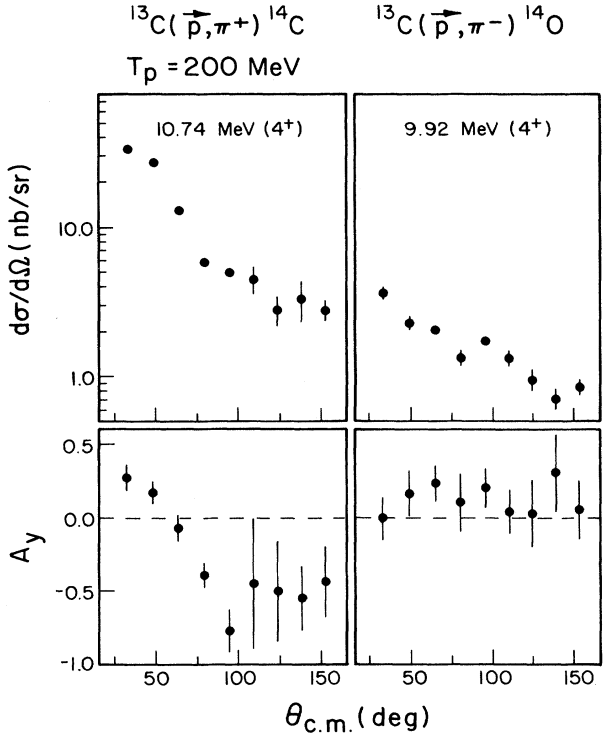

FIG. 8. Cross-section and analyzing power angular distributions for the $^{13}C(p,\pi^{\pm})$ transitions to the 4^+ states at 10.74 MeV in ^{14}C and 9.92 MeV in ^{14}O.

3. 4^+ states in ^{14}C and ^{14}O

As anticipated in Table I, the known 4^+ states at 10.74 MeV in ^{14}C and 9.92 MeV in ^{14}O are seen in our $(p,\pi^{\pm})$ spectra (Fig. 1), although the former is very weak compared to surrounding transitions. These states are widely believed (see Ref. 38, for example) to correspond predominantly to the mirror configurations $|^{12}C\otimes(\nu d_{5/2})^2\rangle$ and $|^{12}C\otimes(\pi d_{5/2})^2\rangle$, which can be reached from the ground state of ^{13}C *only* through the mirror channels $pn\rightarrow nn\pi^+$ and $pn\rightarrow pp\pi^-$, respectively. This observation accounts for the relative weakness of the (p,π^+) transition; as can be seen in Fig. 8, the cross section for the 10.74-MeV state is about an order of magnitude smaller than those for other high-spin (p,π^+) transitions (e.g., 3^-, 4^-, and 5^-), presumably reflecting the relative strength between the free isospin channels σ_{10} vs $(\sigma_{11}+\sigma_{01})$. Within this framework, it is not surprising that $A_y(\theta)$ for the 10.74-MeV state (see Fig. 8) deviates from the typical $(\vec{p},\pi^+)$ A_y pattern exhibited by the continuum and most strong transitions, since in the 4^+ case σ_{10} processes should not play a dominant role.

The case of these 4^+ mirror states in ^{14}C and ^{14}O, which are presumably reached by mirror $NN\rightarrow NN\pi$ channels, offers, in principle, an ideal situation to study nominally identical $NN\rightarrow NN\pi$ processes inside the nucleus. Such a comparison may be complicated, however, by even very small admixtures in the ^{14}C 4^+ wave function of other configurations (e.g.,

$$|^{12}C\otimes(\nu p_{1/2})(\nu f_{7/2})\rangle_{4^+})$$

accessible in (p,π^+) via the dominant σ_{10} channel. Even in the absence of such admixtures the $\pi^+-\pi^-$ comparison is not trivial. The charge-symmetry operation which relates $pn\rightarrow nn\pi^+$ to $pn\rightarrow pp\pi^-$ introduces a reflection of the differential cross section about $\theta_{c.m.}=90°$ (with respect to the incident *proton* momentum) in the two-nucleon center-of-mass frame. In a nuclear transition, this reflection must be folded with the kinematic transformation to the nucleon-nucleus frame and with the dependence of the nuclear form factors on momentum transfer. The analyzing power relationship is furthermore unclear because charge symmetry relates $\vec{p}n\rightarrow nn\pi^+$ to $p\vec{n}\rightarrow pp\pi^-$, whereas we measure with the *proton* polarized in both cases. In light of these complications, differences between the results of these two mirror transitions, such as those seen in Fig. 8, are not surprising.

4. $^{13}C(\vec{p},\pi^{\pm})$ transitions to other discrete states

The advantages offered by the study of mirror *high-spin* states in ^{14}C and ^{14}O are often missing in $(p,\pi^{\pm})$ comparisons involving lower angular momentum transfers. Nonetheless, results for such transitions should also be understood in any comprehensive picture of $^{13}C(p,\pi^{\pm})$. In this section, we present cross-section and analyzing power angular distributions for $^{13}C(\vec{p},\pi^{\pm})$ transitions to some known lower-lying ($E_x<11$ MeV) ^{14}C

and ^{14}O states, along with Kurath's[16] predictions for some of the $^{13}C(p,\pi^+)$ transitions. Other $^{13}C(p,\pi^\pm)$ transitions to states not previously identified at $E_x > 11$ MeV are also briefly discussed.

Figure 9 shows the cross-section and analyzing power angular distributions for some low-lying ^{14}C states populated in $^{13}C(\vec{p},\pi^+)$. Three $d\sigma/d\Omega(\theta)$ patterns can be roughly distinguished here—one involving a deep minimum near $\theta_{c.m.} \simeq 80°$, a second with sharp forward peaking and a shallow minimum near 100°, and a third characterized by a monotonic decrease with increasing momentum transfer—but with no obvious correlation between the pattern exhibited and the quantum numbers of the final states. For most of these states, the 2p1h transition underlying (p,π^+) would not be unique: these wave functions typically comprise two or more different configurations with substantial amplitudes.[12] Also, as was discussed above, single-particle final configurations (with respect to ^{13}C) can be populated through a variety of 2p1h amplitudes (see Table II). In order to see whether these interfering amplitudes may be responsible for the variety of angular distribution shapes observed, one may consider Kurath's calculations,[15,16] which combine the basic two-nucleon coupling $(pp \rightarrow d\pi^+)$ with realistic shell-model wave functions. The calculated $d\sigma/d\Omega(\theta)$, again with one overall normalization factor (the same as used in Fig. 5) applied, are compared to the measurements for four transitions in Fig. 9.

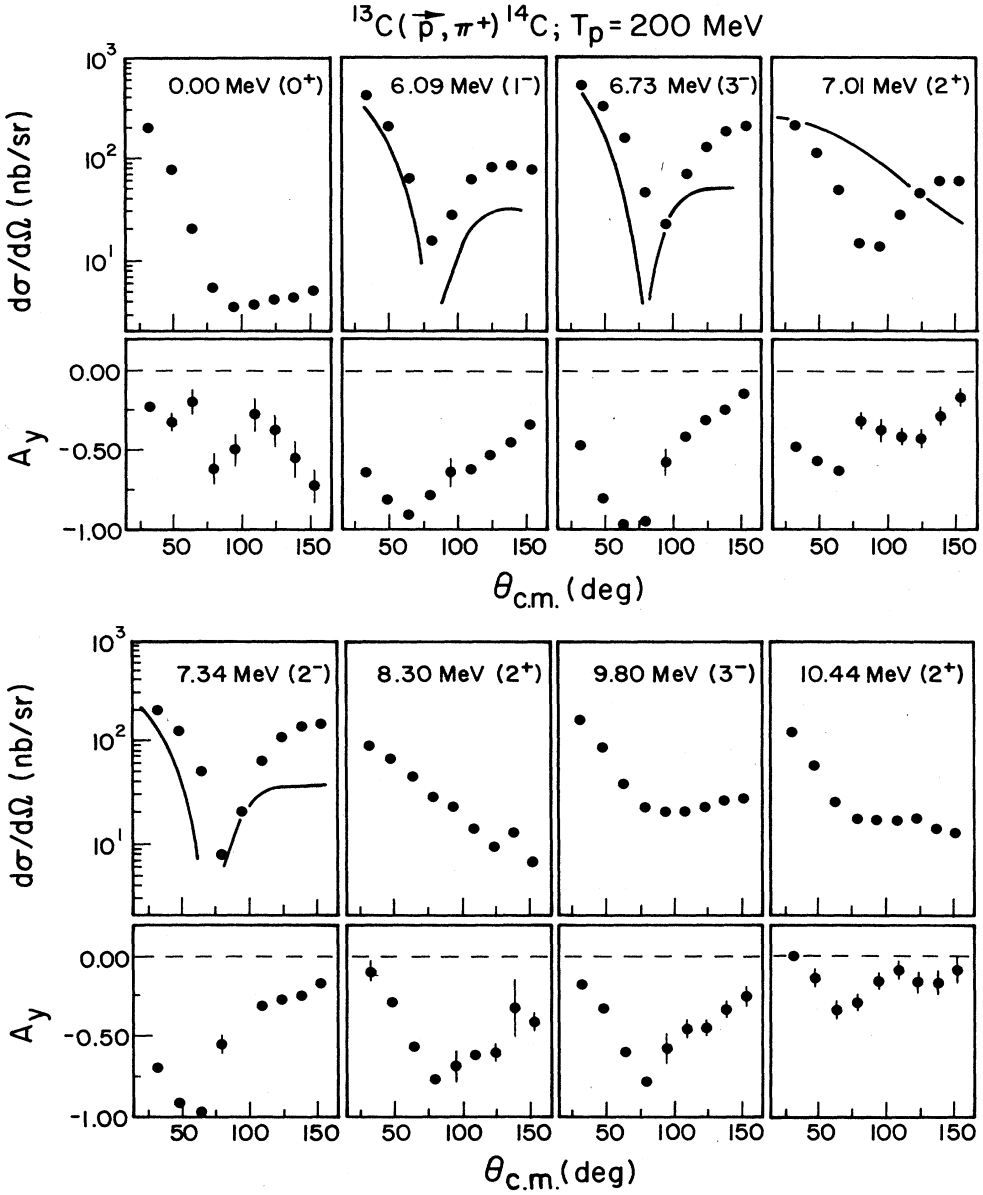

FIG. 9. Cross-section and analyzing power angular distributions for the $^{13}C(p,\pi^+)$ transitions to the ^{14}C states at 0.0 (0^+), 6.09 (1^-), 6.73 (3^-), 7.01 (2^+), 7.34 (2^-), 8.30 (2^+), 9.80 (3^-), and 10.44 (2^+) MeV. Shown by the solid curves are Kurath's calculations for some of these transitions (Ref. 16).

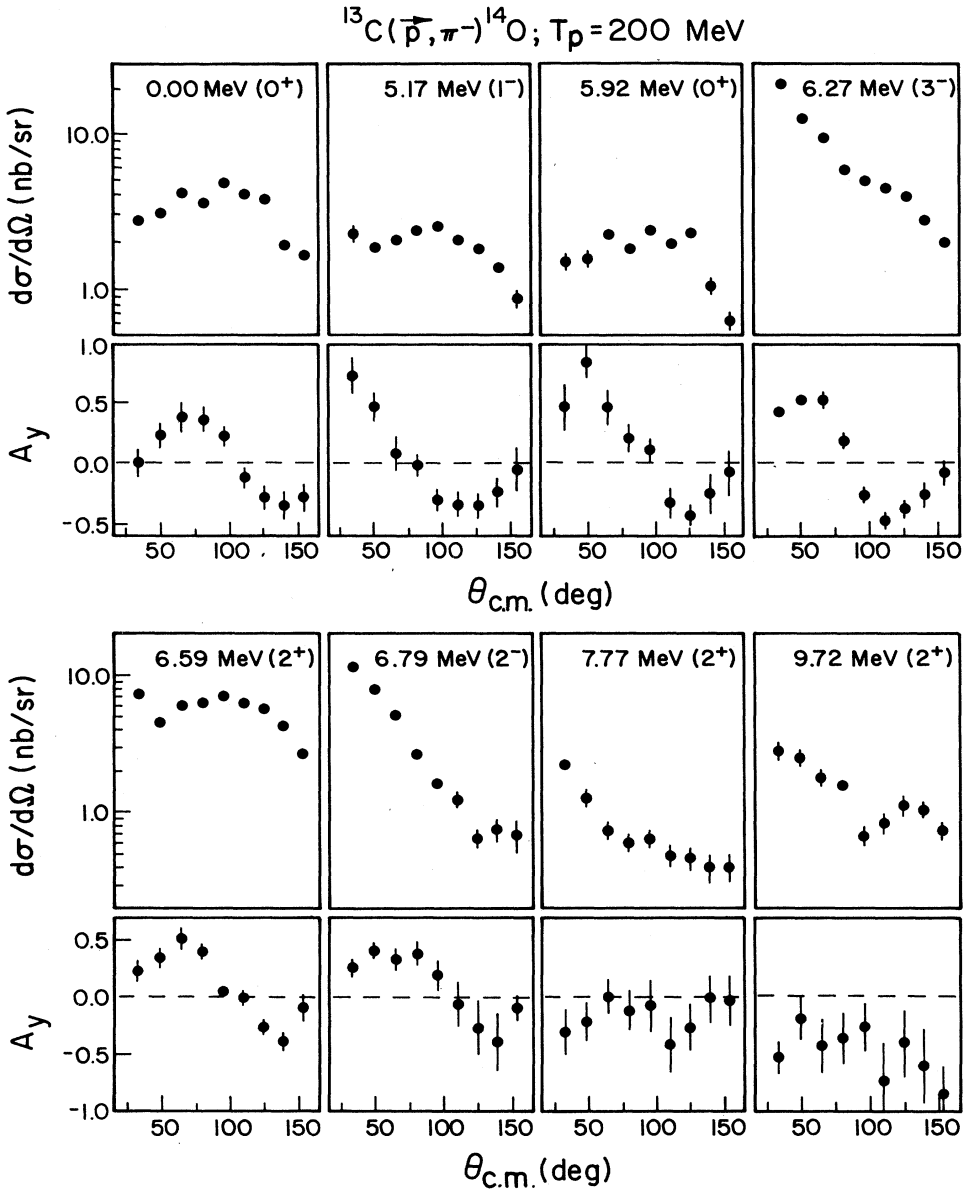

FIG. 10. Cross-section and analyzing power angular distributions for the $^{13}C(p,\pi^-)$ transitions to the ^{14}O states at 0.0 (0^+), 5.17 (1^-), 5.92 (0^+), 6.27 (3^-), 6.59 (2^+), 6.79 (2^-), 7.77 (2^+), and 9.72 (2^+) MeV.

The *calculations* in Fig. 9 exibit two distinct types of angular distribution patterns. The ones with sharp minima result[15] from destructive interferences between one-body and two-body amplitudes for transitions leading to final states having appreciable single-particle components in their wave functions. In contrast, the calculated cross section falls monotonically for transitions—such as those for the 4^- and 5^- states considered previously (Fig. 5)—with only 2p1h components in the final-state wave functions. For the states in the first class in Fig. 9, the calculations qualitatively reproduce the observed relative strengths and the observed minima, given that the depth and precise location of the calculated minima are certainly influenced[15] by the neglect of proton and pion distortions. On the other hand, the calculated angular distribution for the 2^+ state in Fig. 9 completely misses the observed minimum for the 7.01-MeV state, although it provides a good match to the observed shape for the *second* 2^+ state at $E_x = 8.30$ MeV. It should be noted that a 2^+ ^{14}C state can have a single-particle configuration with respect to ^{13}C only if one includes either *fp*-shell excitations or 2p2h admixtures in the ^{13}C ground state, both of which are neglected in the calculations performed by Kurath.

In the analyzing power angular distributions shown in Fig. 9, one can easily discern the typical $(\vec{p},\pi^+)$ A_y pat-

tern exhibited by the continuum (Sec. III A) and by the high-spin 4^- and 5^- states (Sec. III B 1) considered previously. Superimposed on this pattern, however, are some appreciable state-to-state variations, for example, the A_y excursion to a less negative value observed for the 2^+ state at 7.01 MeV near the cross-section minimum ($\sim 80°$). Another variation is exhibited by the ground-state transition, for which the interacting *spin* system is especially simple ($\frac{1}{2}+\frac{1}{2}\rightarrow 0+0$), thus highly constraining the entrance- and exit-channel partial waves (see Ref. 17 for a full discussion). Taken together, these results suggest, again, the dominance of the σ_{10} $NN\rightarrow NN\pi$ amplitude in most strong (p,π^+) transitions.

The (p,π^-) cross-section angular distributions for the low-spin ^{14}O states at $E_x<11$ MeV are shown in Fig. 10. These states, except for the 0^+ state at 5.92 MeV, are the mirrors of the ^{14}C states of Fig. 9 (the ^{14}C 0^+ excited state being unresolved from other transitions). Note that there seems to be no appreciable ^{13}C(p,π^-) population of an ^{14}O state mirroring the 3^- ^{14}C state at 9.8 MeV. This is not surprising since such a state would have[12] the dominant configuration

$$|^{12}\mathrm{C}\otimes(\pi p_{1/2})^2_{0^+}(p_{3/2})^{-1}(d_{5/2})\rangle \ ,$$

which is not accessible via a 2p1h $(pn\rightarrow pp\pi^-)$ transition from the ground state of ^{13}C. Once again, there is no simple correlation between the nature of the observed angular distribution pattern and the quantum numbers of the final nuclear states. In (p,π^-) transitions, there are no one-body amplitudes analogous to those responsible for the deep interference minima in some calculated (p,π^+) angular distributions. Furthermore, knowledge of the final-state configuration uniquely determines the 2p1h shell-model rearrangement responsible for the transition. However, most of the states considered in Fig. 10 again comprise two or more different accessible configurations.[12]

The analyzing power angular distributions for the ^{14}O states are also shown in Fig. 10. Here the qualitative character of the $A_y(\theta)$ results for discrete states deviates more strongly from the continuum $A_y(\theta)$ [see Fig. 3(a)] than in $(\vec{p},\pi^+)$.

Other ^{14}C and ^{14}O discrete states at $E_x>11$ MeV are populated appreciably in ^{13}C$(p,\pi^\pm)$. As shown in the spectra of Fig. 1, these states are relatively weaker than the high-spin states already discussed, *except* for the 23.2-MeV state in ^{14}C, which will be treated in Sec. III D. Figure 11 shows the $d\sigma/d\Omega$ and A_y angular distributions for the ^{13}C(p,π^+) peaks observed at $E_x=12.96$ and 13.56 MeV. The typical $(\vec{p},\pi^+)$ $A_y(\theta)$ behavior is clearly observed for these states, confirming once more the dominance of σ_{10} processes. The 12.96-MeV state has been seen previously as a narrow resonance in a ^{13}C(n,n') study,[39] and a tentative spin-parity assignment of 3^- has been suggested for it from the results of a ^{14}C(α,α') study.[40] The 13.56-MeV state, however, is not known from any previous work.

Figure 12 shows the $d\sigma/d\Omega$ and A_y angular distributions for the ^{14}O states observed in ^{13}C(p,π^-) at $E_x=11.97$, 14.60, and 17.36 MeV. States at these excitation energies have been observed in the ^{14}N$(^3$He$,t)^{14}$O study of Ref. 37, but nothing has been reported about their possible identities. Compared to the other ^{13}C(p,π^-) transitions, $d\sigma/d\Omega(\theta)$ for the 11.97-MeV state, for instance, resembles most closely that for the strong state at 14.15 MeV (see Fig. 6), which we have tentatively identified as the 5^- mirror of the 14.87-MeV state in ^{14}C.

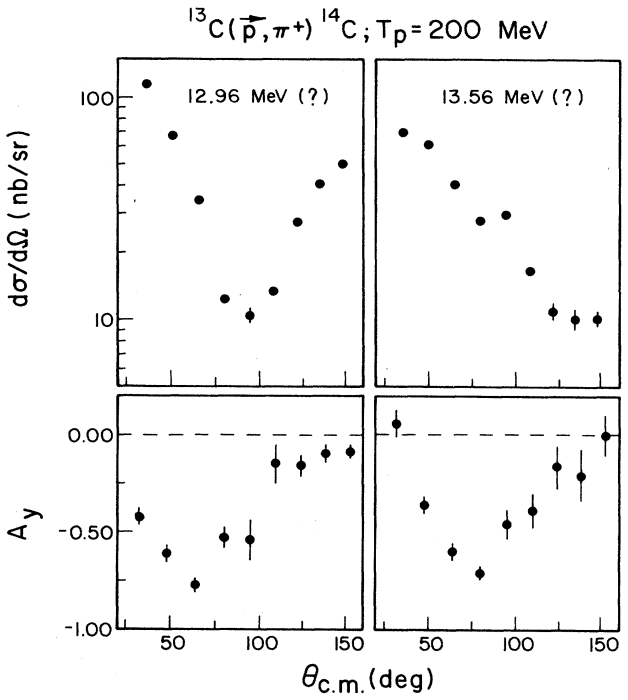

FIG. 11. Cross-section and analyzing power angular distributions for the ^{13}C(p,π^+) transitions to the ^{14}C states at 12.96 and 13.56 MeV.

C. ^{12}C$(\vec{p},\pi^+)$ transitions to discrete ^{13}C states

The ^{12}C$(p,\pi^+)^{13}$C reaction has been studied previously[1,17,33] at $T_p=200$ MeV. Cross sections and analyzing powers have been measured[1,17] for low-lying final states ($E_x<4$ MeV) and cross sections alone have been reported[33] for states up to 10-MeV excitation. The measurements presented in this paper include, however, $d\sigma/d\Omega(\theta)$ and $A_y(\theta)$ for final states up to ~ 22 MeV in excitation energy. A typical ^{12}C(p,π^+) spectrum at $\theta_{lab}=30°$ is shown in Fig. 1. In this spectrum, strong ^{13}C states (or groups of states) are identified at $E_x=0.0$, 3.09, (3.68+3.85), 6.86, (7.49+7.55+7.69), 9.5, and 21.4 MeV. The latter transition, and its similarities to that in ^{13}C(p,π^+) leading to the strong state at $E_x=23.2$ MeV, are the main focus of the present ^{12}C$(\vec{p},\pi^+)$ study. Before discussing the results for these high-lying states in Sec. III D, we present here a brief discussion of the general features exhibited by the lower-lying ^{13}C states, along with some theoretical calculations.

The cross-section and analyzing power angular distri-

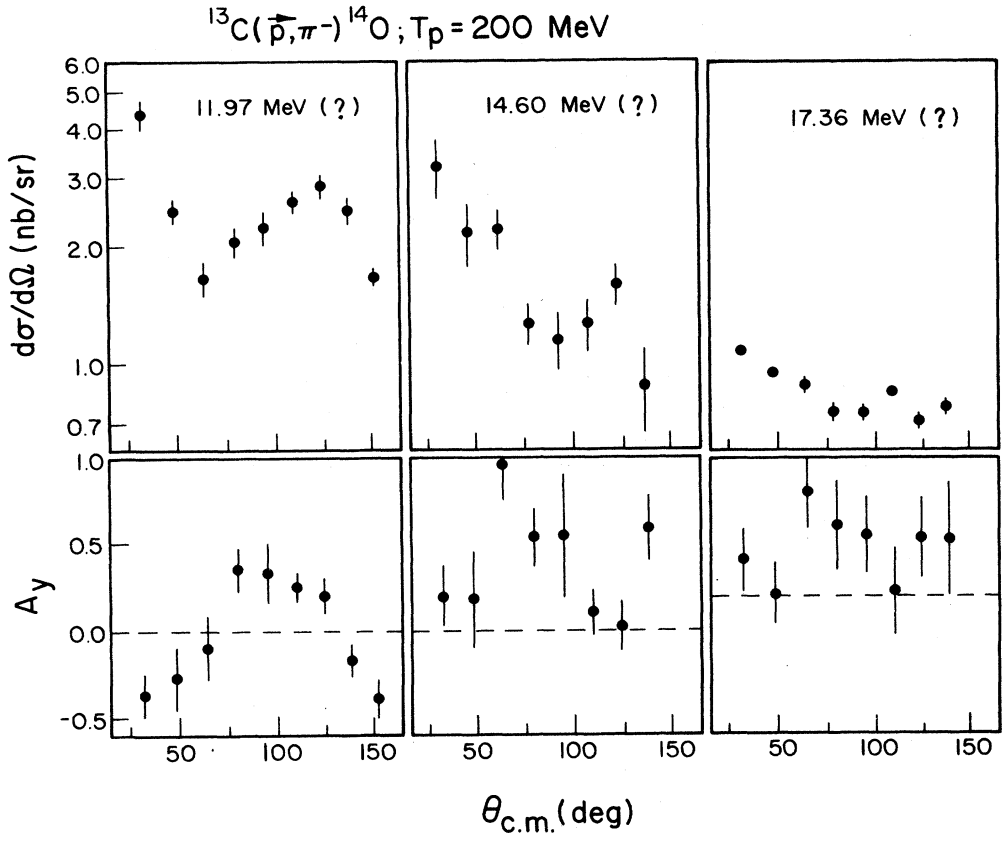

FIG. 12. Cross-section and analyzing power angular distributions for the $^{13}C(p,\pi^-)$ transitions to the ^{14}O states at 11.97, 14.60, and 17.36 MeV.

butions for the strong $^{12}C(p,\pi^+)$ peaks observed at $E_x < 10$ MeV are shown in Fig. 13. Some of these peaks, as noted above and in Fig. 13, actually comprise two (or more) unresolved states. The present $d\sigma/d\Omega$ measurements in Fig. 13 agree with those of Ref. 33 to within an overall normalization difference of $\sim 15\%$, which is the level of the systematic uncertainty associated with the present absolute cross-section measurements.

Kurath's calculations[15] for these low-lying transitions reproduce some of the qualitative features observed in Fig. 13. In addition to the overall level of agreement discussed in Ref. 15, we note in association with our data the reasonable agreement achieved for the 7.6-MeV complex, for which the calculations suggest a very small cross-section contribution from the $\frac{7}{2}^+$ state and a dominant contribution from the $\frac{5}{2}^-$ state. A major discrepancy between the data and the calculations concerns the $\frac{5}{2}^+$ state at 6.86 MeV: while calculations qualitatively explain the *relative* strengths for most observed states, they predict[15] for this 6.86-MeV state a much smaller cross section (not shown in Fig. 13) than experimentally observed.

In the analyzing power results shown in Fig. 13, one clearly notes again the almost universal underlying $(\vec{p},\pi^+)$ $A_y(\theta)$ pattern. For the ground $(\frac{1}{2}^-)$ and 3.09-MeV $(\frac{1}{2}^+)$ states, where the simple spin system $(\vec{\frac{1}{2}}+\vec{0}\rightarrow\vec{\frac{1}{2}}+\vec{0})$ severely constrains the contributing partial waves, there are significant excursions in $A_y(\theta)$ near the cross-section minima. These have been considered in Ref. 17.

D. The $(\vec{p},\pi^+)$ results for the states at $E_x=23.2$ MeV in ^{14}C and 21.4 MeV in ^{13}C

The highly excited strong states observed in $^{13}C(p,\pi^+)^{14}C$ at $E_x=23.2$ MeV and in $^{12}C(p,\pi^+)^{13}C$ at $E_x=21.4$ MeV (see Fig. 1) exhibit anomalous behavior in comparison with the other transitions studied. As can be seen in Fig. 14, their cross sections are comparable in magnitude to those of the strongest $^{12,13}C(p,\pi^+)$ transitions to lower-lying states, but their analyzing powers are nearly zero at all angles. These states represent, therefore, the only *strong* $^{12,13}C(p,\pi^+)$ transitions whose analyzing power deviates dramatically from the typical $A_y(\theta)$ pattern followed by all other strong (p,π^+) transitions that apparently proceed predominantly via $pp\rightarrow(np)_{T=0}\pi^+$ processes.

The ^{14}C state at $E_x=23.2$ MeV is not known from any previous work, but a state at this excitation is populated

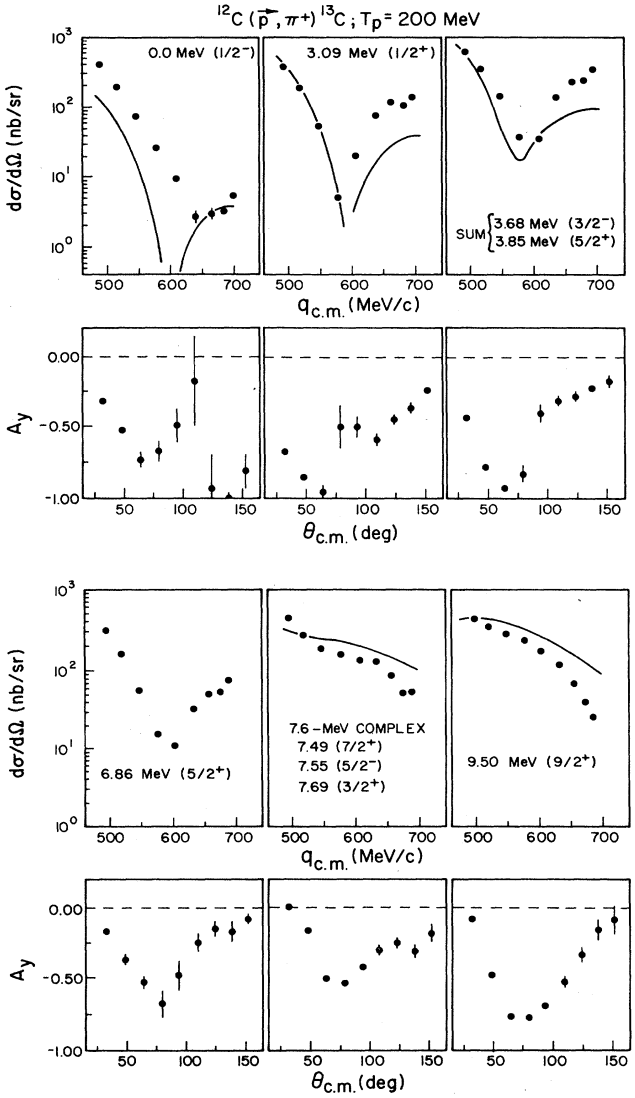

FIG. 13. Cross-section and analyzing power angular distributions for the $^{12}C(p,\pi^+)$ transitions to the ^{13}C states at 0.0 ($\frac{1}{2}^+$), 3.09 ($\frac{1}{2}^-$), 3.68 ($\frac{3}{2}^-$)+3.85 ($\frac{5}{2}^+$), 6.86 ($\frac{5}{2}^+$), 7.49 ($\frac{7}{2}^+$)+7.55 ($\frac{5}{2}^-$)+7.69 ($\frac{3}{2}^+$), and 9.5 ($\frac{9}{2}^+$) MeV. Shown by the solid curves are Kurath's calculations for some of these transitions (Ref. 15).

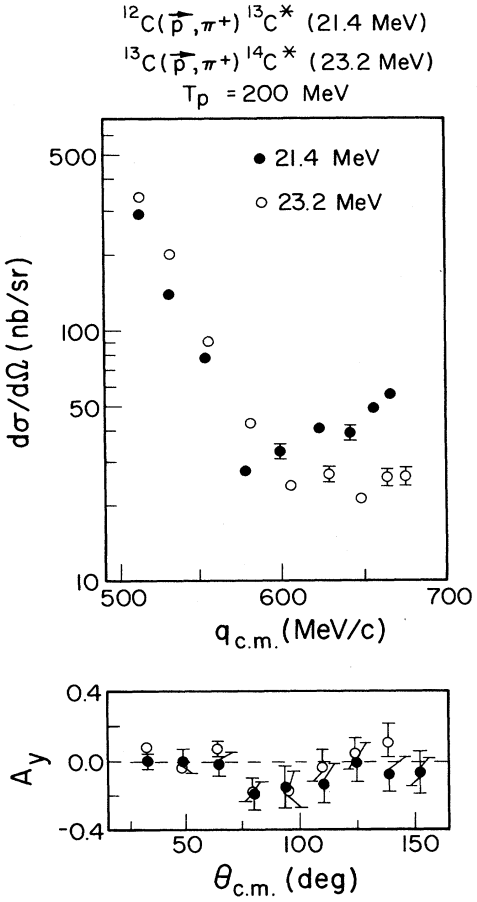

FIG. 14. Cross-section and analyzing power angular distributions for the $^{12}C(p,\pi^+)$ transition to the ^{13}C state at 21.4 MeV and the $^{13}C(p,\pi^+)$ transition to the ^{14}C state at 23.2 MeV.

weakly in a back-angle $^{14}C(e,e')$ spectrum,[41] with a strength more typical of natural-parity than of unnatural-parity transitions. The ^{13}C state coincides in excitation energy with an $M4$ transition observed[35,13] in $^{13}C(\pi,\pi')$ and $^{13}C(e,e')$, suggesting a dominant

$$|^{13}C\otimes[(p_{3/2})^{-1}(d_{5/2})]_{4^-}\rangle$$

configuration with $J^\pi=\frac{7}{2}^+$ or $\frac{9}{2}^+$. Comparison of $(\pi^+,\pi^{+'})$ to $(\pi^-,\pi^{-'})$ cross sections suggests[35] that the peak observed near $E_x=21.5$ MeV in $^{13}C(\pi^\pm,\pi^{\pm'})$ at $T_\pi=165$ MeV may be isospin mixed ($T=\frac{1}{2}$ and $\frac{3}{2}$), based on the known $(\pi^++N)/(\pi^-+N)$ free cross-section ratios near the Δ resonance. Shell-model calculations[34] suggest several candidate states in this vicinity for such an $M4$ excitation, with $J^\pi=\frac{7}{2}^+$ or $\frac{9}{2}^+$ and $T=\frac{1}{2}$ or $\frac{3}{2}$.

The similarity observed in (p,π^+) results between these two transitions (see Fig. 14) in excitation energy, cross section, and analyzing power suggests that the final states are of similar structure. One possible explanation for these anomalous states that would be at least qualitatively consistent with their excitation energies, their observed widths, and the above inelastic scattering and shell-model results, would be that they are $T_>$ states of moderate spin [e.g.,

$$|^{12}C\otimes(\nu p_{1/2})(p_{3/2})^{-1}(p_{1/2})(d_{5/2}))\rangle_{3^-,T=2}$$

in ^{14}C and

$$|^{12}C\otimes(p_{3/2})^{-1}(p_{1/2})(d_{5/2}))\rangle_{7/2^+,T=3/2}$$

in ^{13}C]. The excitation energy of the ^{14}C state at 23.2 MeV is indeed about right for a 3^-, $T=2$ state, based on tentative spin-parity assignments[32] for low-lying states in

the isobaric nuclide ^{14}B. Such a $T=2$ state in ^{14}C would have only a single open isospin-conserving decay channel (to $^{13}B_{g.s.}+p+2.4$ MeV), accounting for the sharpness of the observed peak (the intrinsic width is estimated from our spectra to be ~ 85 keV). In contrast, at $T=\frac{3}{2}$ excitation at 21.4 MeV in ^{13}C would have several open isospin-conserving partial decay channels—neutron decay to $T=1$ states in ^{12}C (1^+, 15.11 MeV and 2^+, 16.1 MeV) and proton decay to $^{12}B_{g.s.}$—accounting for its relatively large inferred intrinsic width (~ 210 keV). Furthermore, such $T_>$ states could be populated *only* via $\Delta T=\frac{3}{2}$ (p,π^+) transitions, to which the σ_{10} isospin channel *cannot* contribute, providing a natural explanation for their anomalous A_y behavior.

The large (p,π^+) cross sections measured for these transitions argue, however, against interpreting these peaks as relatively pure $T_>$ states, since the relevant free σ_{11} and σ_{01} $NN\rightarrow NN\pi$ channels are very weak near threshold, so that one should expect quite weak $\Delta T=\frac{3}{2}$ (p,π^+) transitions. It should be kept in mind that these isospin channels dominate (p,π^-) reactions, but that (p,π^-) cross sections are typically an order of magnitude weaker than those for (p,π^+), in general agreement with expectations based on free $NN\rightarrow NN\pi$ results. The absence in Fig. 1 of a similarly strong mirror $^{13}C(p,\pi^-)$ excitation argues even more convincingly against this pure $T_>$ interpretation, as isospin conservation requires *equal* $^{13}C(p,\pi^{\pm})$ cross sections for mirror $T=2$ states, where transitions would have to proceed through a pure $(T_{tot}=1, T_3=0)$ overall isospin channel.[24]

It is more plausible, therefore, to interpret these states as isospin mixed, but having the same configurations and spins as those mentioned above. A sizable, but not necessarily dominant $T_<$ admixture in the wave function would introduce a $\Delta T=\frac{1}{2}$ contribution to the transition amplitude—and hence, probably a strong enhancement in the cross section—for $^{12,13}C(p,\pi^+)$, but not for $^{13}C(p,\pi^-)$ to a mirror state, since *all* (p,π^-) transitions involve $\Delta T=\frac{3}{2}$. In addition to explaining the large cross sections observed, such isospin mixing would also make the anomalous A_y behavior less of a mystery: for such (p,π^+) transitions, $A_y(\theta)$ might well fall in between the negative ($\Delta T=\frac{1}{2}$) and positive ($\Delta T=\frac{3}{2}$) values [observed for the $^{13}C(p,\pi^{\pm})$ continuous, see Fig. 3] typifying the coherent contributing amplitudes. This isospin-mixing scenario would be supported by the $^{13}C(\pi^{\pm},\pi^{\pm'})$ results[35] mentioned above.

These states could alternatively be $T_<$ states of sufficiently high spin to suppress their particle decay strongly. They would then be inaccessible via (e,e') or (π,π'), and so would have to *accidentally* overlap the states observed in (e,e') and (π,π'). For instance, "stretched" (maximum angular momentum coupling) configurations of the form

$$|^{13}C\otimes(\pi p_{3/2})^{-1}(\pi d_{5/2})(\nu d_{5/2})\rangle_{7^+}$$

in ^{14}C and

$$|^{12}C\otimes(\pi p_{3/2})^{-1}(\pi d_{5/2})(\nu d_{5/2})\rangle_{13/2^-}$$

in ^{13}C would be reachable via the strong σ_{10} channels. The expected excitation energies of such states can be estimated in weak-coupling calculations,[42] which predict E_x(weak coupling)$\simeq 23.47$ MeV for the 7^+ in ^{14}C (consistent with the observed peak), but 18.8 MeV for the $\frac{13}{2}^-$ in ^{13}C. The deviant A_y behavior for these states might then be characteristic of the extreme angular momentum coupling of the two particles and one hole. One should expect, in general, that the intrinsic A_y signature of the underlying $pp\rightarrow d\pi^+$ process may have superimposed upon it contributions arising from distortion-induced "sidedness,"[2] i.e., from a preference for interacting with a target proton on one or the other side of the target nucleus. Such contributions are expected to become more pronounced when the coupling of the target nucleon's spin and orbital angular momentum is most highly constrained. Indeed, analogous $(\vec{p},\pi^-)$ transitions to *stretched* 2p1h final states appear to exhibit[6,7] a universal $A_y(\theta)$ signature distinct from the results for lower-spin states.

Further experiments to elucidate the nature of these ^{13}C and ^{14}C anomalous states, with their possible implications for the (p,π^+) reaction mechanism, have been initiated. A study of the $^{11}B(\alpha,p)$ and $^{11}B(\alpha,d)$ reactions, searching for high-spin $T_<$ states at high excitation energies in ^{14}C and ^{13}C, has just been completed.[43] We have also recently performed a $^{12}C(p,\pi^+n)$ coincidence experiment, aimed at constraining the isospin of the 21.4-MeV state in ^{13}C by searching for its neutron decay to $T=1$ vs $T=0$ daughter states.[44] In addition, we mention recent studies[45] searching for similar anomalous (p,π^+) transitions to high excitations in other *p*- or *sd*-shell nuclei (^{15}N, ^{16}N, and ^{17}O). The results (to be reported elsewhere) of the studies mentioned above are, unfortunately, as yet inconclusive regarding the quantum numbers or configurations of the anomalous ^{13}C and ^{14}C states.

IV. CONCLUSIONS

The $^{13}C(\vec{p},\pi^{\pm})$ and $^{12}C(\vec{p},\pi^+)$ results presented in this paper provide evidence suggesting the dominance of a quasifree TNM in near-threshold $A(p,\pi^{\pm})A+1$ reactions. The quasifree nature of $NN\rightarrow NN\pi$ inside the nuclear medium is most strongly supported by comparison of the observed $^{13}C(\vec{p},\pi^+)$ *continuum* $A_y(\theta)$ to experimental results for the free $\vec{p}p\rightarrow d\pi^+$ (i.e., σ_{10}) process. Also, the $^{13}C(\vec{p},\pi^-)$ continuum analyzing powers were compared to $A_y(\theta)$ *predictions* for $\vec{p}n\rightarrow(pp)^1S_0\pi^+$, based on a phase-shift analysis of measured differential cross sections for π^- absorption on the two-proton pair in ^3He. The comparison favors the dominance of a specific (σ_{01}) amplitude $[(pn)^3D_1, T=0\rightarrow(pp)^1S_0\pi^-]$, not involving a ΔN intermediate state in the π^- absorption/creation process, and suggests the quasifree nature of $pn\rightarrow pp\pi^-$ underlying (p,π^-) reactions on nuclei. Direct measurements of the free $\vec{p}n\rightarrow pp\pi^-$ analyzing power near threshold are needed to support this conclusion (such measurements have, in fact, already been initiated at TRIUMF, Ref. 46). In addition, we have shown that the relative strengths of the various free $NN\rightarrow NN\pi$ isospin

channels appear to be maintained inside the nucleus.

The experimental results for selected ^{14}C and ^{14}O high-spin mirror states populated in $^{13}C(p,\pi^{\pm})$ are consistent with the dominance of $pp \rightarrow (pn)_{T=0}\pi^+$ in (p,π^+) and of $pn \rightarrow pp\pi^-$ in (p,π^-). On the basis of qualitative TNM arguments and comparison to other reaction studies, we were able to make some spectroscopic applications, the most interesting of which were $J^{\pi}=5^-$ assignments to states near $E_x \simeq 15$ MeV in ^{14}C and ^{14}O. The cross-section angular distributions for some $^{12,13}C(p,\pi^+)$ transitions were compared to simple theoretical calculations in which only the $pp \rightarrow d\pi^+$ channel is included. These calculations emphasize the effect of nuclear wave functions on the (p,π^+) reaction, and provide at least a qualitative understanding of the relative strengths and angular distribution shapes for various strong transitions.

The observations for $^{12,13}C(\vec{p},\pi^+)$ transitions to a 21.4-MeV state in ^{13}C and a 23.2-MeV state in ^{14}C prompted further investigation. These transitions exhibit striking deviations from the typical empirical patterns followed by the analyzing power for the continuum and for all other *strong* (p,π^+) transitions studied. Two alternative interpretations were suggested for these states: qualitative arguments consistent with the observed excitation energies, widths, and strengths of these (p,π^+) peaks, but allowing anomalous A_y behavior within a TNM context, were offered for isospin-mixed states of moderate spin and for $T_<$ states with stretched angular momentum coupling for 2p1h excitations within the *p* and *sd* shells. Ongoing experimental investigations aimed at testing these interpretations were briefly described.

Theoretical efforts to understand existing $(p,\pi^{\pm})$ data in two-nucleon models are continuing.[10] Only through a successful microscopic description may the $A(p,\pi)$ reaction be fully and quantitatively understood. It is important that the assumptions made in such calculations be consistent with reaction features suggested by the data themselves. In particular, the role of nonresonant contributions (i.e., no ΔN intermediate state) to $pn \rightarrow pp\pi^+$ processes inside nuclei must be considered in light of the agreement we have reported between measured $A(\vec{p},\pi^-)$ continuum analyzing powers and expectations for σ_{01}-dominated two-nucleon amplitudes.

We would like to thank Dr. D. Kurath for the results of his $^{13}C(p,\pi^+)$ calculations which he made available to us along with very useful comments.

---

*Present address: TRIUMF, 4004 Wesbrook Mall, Vancouver, B.C., Canada V6T 2A3.

†Present address: Department of Physics, State University of New York at Stony Brook, Stony Brook, NY 11794.

‡Present address: LeCroy Research Systems, Spring Valley, NY 10977.

[1]E. G. Auld *et al.*, Phys. Rev. Lett. **41**, 462 (1978).
[2]W. W. Jacobs *et al.*, Phys. Rev. Lett. **49**, 855 (1982).
[3]S. E. Vigdor *et al.*, Phys. Rev. Lett. **49**, 1314 (1982).
[4]S. E. Vigdor *et al.*, Nucl. Phys. **A396**, 61c (1983).
[5]B. A. Brown *et al.*, Phys. Rev. Lett. **51**, 1952 (1983).
[6]M. C. Green *et al.*, Phys. Rev. Lett. **53**, 1893 (1984).
[7]T. G. Throwe *et al.*, Phys. Rev. C **35**, 1083 (1987).
[8]O. Scholten *et al.*, Phys. Rev. C **32**, 653 (1985); O. Scholten and H. Toki, *ibid.* **34**, 601 (1986).
[9]R. D. McKeown *et al.*, Phys. Rev. Lett. **44**, 1033 (1980).
[10]See, for example, M. J. Iqbal and G. E. Walker, Phys. Rev. C **32**, 556 (1985); P. W. F. Alons *et al.*, Nucl. Phys. **A480**, 413 (1988).
[11]S. Cohen and D. Kurath, Nucl. Phys. **73**, 1 (1965).
[12]S. Lie, Nucl. Phys. **A181**, 517 (1972).
[13]R. A. Lindgren, J. Phys. (Paris) Colloq. **45**, C4, 433 (1984).
[14]D. B. Holtkamp *et al.*, Phys. Rev. C **31**, 957 (1985).
[15]D. Kurath, Phys. Rev. C **35**, 2247 (1987).
[16]D. Kurath (private communication).
[17]M. C. Green, Ph.D. thesis, Indiana University, 1983.
[18]P. H. Pile, Ph.D. thesis, Indiana University, 1978.
[19]B. J. Verwest and R. A. Arndt, Phys. Rev. C **25**, 1979 (1982).
[20]R. P. Redwine, Nucl. Phys. **A434**, 239c (1985), and references therein.
[21]G. Jones, in *Pion Production and Absorption in Nuclei–1981* (Indiana University Cyclotron Facility), Proceedings of the Conference on Pion Production and Absorption in Nuclei, AIP Conf. Proc. No. 79, edited by R. D. Bent (AIP, New York, 1982), p. 13.
[22]W. R. Falk *et al.*, Phys. Rev. C **32**, 1972 (1986).
[23]S. M. Aziz, Ph.D. thesis, Indiana University, 1988 (unpublished).
[24]E. Korkmaz *et al.*, Phys. Rev. Lett. **58**, 104 (1987).
[25]J. J. Kehayias *et al.*, Phys. Rev. C **33**, 1388 (1986).
[26]T. D. S. Stanislaus, Ph.D. thesis, University of British Columbia, 1987.
[27]M. A. Moinester *et al.*, Phys. Rev. Lett. **52**, 1203 (1984).
[28]E. Piasetsky *et al.*, Phys. Rev. Lett. **57**, 2135 (1986).
[29]S. E. Vigdor *et al.*, Phys. Rev. Lett. **58**, 840 (1987).
[30]J. A. Niskanen, Nucl. Phys. **A298**, 417 (1978).
[31]M. A. Moinester *et al.*, Phys. Rev. Lett. **58**, 841 (1987).
[32]F. Ajzenberg-Selove, Nucl. Phys. **A449**, 1 (1986), and references therein.
[33]F. Soga *et al.*, Phys. Rev. C **24**, 570 (1981).
[34]T.-S. H. Lee and D. Kurath, Phys. Rev. C **22**, 1670 (1980).
[35]S. J. Seestrom-Morris *et al.*, Phys. Rev. C **26**, 594 (1982).
[36]Kurath's calculations, described in Ref. 15, assume an *s*-wave π^+-*d* final state in the underlying $pp \rightarrow d\pi^+$ process, while phase-shift analyses (see, e.g., Ref. 30) indicate that the dominant amplitudes are associated with *p*-wave π-*d* states in the free *pp* interaction. It is not clear how much the *s*-wave assumption affects the qualitative conclusions we draw from Kurath's calculations.
[37]G. C. Ball and J. Cerney, Phys. Rev. **177**, 1466 (1969).
[38]H. T. Fortune *et al.*, Phys. Rev. Lett. **40**, 1236 (1978).
[39]R. O. Lane *et al.*, Phys. Rev. C **23**, 1883 (1981).
[40]R. J. Peterson *et al.*, Nucl. Phys. **A425**, 469 (1984).
[41]M. A. Plum *et al.*, Nucl. Phys. **137B**, 15 (1984).
[42]R. Sherr *et al.*, Phys. Lett. **52B**, 401 (1974).
[43]J. D. Brown *et al.*, Phys. Rev. C **38**, 1958 (1988).
[44]E. Korkmaz *et al.*, Indiana University Cyclotron Facility Scientific and Technical report, 1986, p. 67; Indiana Universi-

ty Cyclotron Facility Scientific and Technical report, 1987, p. 65; E. Korkmaz, Ph.D. thesis, Indiana University, 1987 (unpublished).

[45]S. M. Aziz *et al.*, Indiana University Cyclotron Facility Scientific and Technical report, 1986, p. 61; Indiana University Cyclotron Facility Scientific and Technical report, 1987, p. 81.

[46]D. A. Hutcheon, P. L. Walden, and M. A. Moinester, TRIUMF Research proposal No. 460, 1987, and extension, 1988.